ACOUSTICAL AIRSPEED INDICATORS

Thesis by

David T. Barish

In Partial Fulfillment of the Requirements

For the Degree of

Aeronautical Engineer

California Institute of Technology

Pasadena, California

1950

ACKNOWLEDGMENTS

The author wishes to express his appreciation to Dr. H. W. Liepmann and to Dr. H. Nagamatsu for the amount of effort they put forth in the guidance of this thesis work.

ABSTRACT

Some of the problems associated with the applications of acoustical devices for the determination of airstream characteristics are considered in this study. The velocity and pressure fields for both point sound sources and finite sound sources in both subsonic and supersonic flow are discussed, with a view toward using sound waves for the determination of velocity, Mach number, temperature, and other properties of a flow.

The experimental investigations included the measurement of the spectra of ultra-audio-pressure pulsations, both static and total, in the small C.I.T. supersonic tunnel and also in the C.I.T. hypersonic tunnel. A broad range of Mach numbers and a variety of operating conditions were covered. The development of a modified Hartmann sound generator is described, and measurements of the sound field from this device in supersonic flow are included.

TABLE OF CONTENTS

		Page
I.	Introduction	1
II.	Discussion of Acoustical Potential Equations	6
	A. Application of Lorentz-Galilean Transformation	6
	B. The Point Source in Subsonic Flow	7
	C. The Point Source in Supersonic Flow	9
	D. The Finite Emitter Problem	11
	E. The Finite Emitter in Supersonic Flow	13
	F. The Two-dimensional Emitter in Supersonic Flow	15
III.	Experimental Program	17
	A. Description of Equipment	17
	1. Massa Sound Probe	17
	2. Wave Analyser	17
	3. Wind Tunnels	18
	4. Flat Plate Model	18
	5. Total Pressure Stand	19
	6. Hartmann Sound Generator	19
	B. Description of Experiments	23
	1. Calibration of Receiver Apparatus	23
	2. Noise Surveys	26
	a. Static Pressure Surveys at Wind Tunnel Wall	27
	b. Static Pressure Surveys with Flat Plate Model	28

TABLE OF CONTENTS (Cont'd)

	Page
c. Total Pressure Surveys	29
3. Sound Field Measurements	29
IV. Conclusions	32

I. INTRODUCTION

The use of acoustical instruments for the measurement of flow parameters has been considered for some years. To the author's knowledge, the first attempt to measure flow velocity with sound waves was initiated by the Cruft Laboratory at Harvard[1] for use on blimps. The unit consisted of a flat plate about 12 inches long with a sound source mounted at the center and a receiver at each streamwise end. The signals from the two receivers were fed to a phase discriminating circuit which gave an indication of the airspeed. The predominant difficulty encountered with this device was due to the fact that an appreciable part of the medium through which the signal was transmitted was in the boundary layer of the plate, and therefore a large correction had to be applied. Elrod[2] has recently written a doctor's thesis concerning this correction.

A more recent study of similar devices was conducted by Cornell Aeronautical Laboratories and Fredric Flader, Inc.[3] during 1947. A rather detailed investigation into possible methods of utilizing sound waves for airspeed determination was conducted. Two methods were considered most feasible. In both of these, the difficulties associated with boundary layers were minimized by placing the emitter on a different surface from the receiver and propagating the sound in a direction

essentially normal to the stream direction. The first, called an "apparent position method" required the production of beamed plane sound waves, the idea being that this beam would be displaced through an angle dependent directly upon the free stream velocity. This method was also considered by Cady[4], but little success has been achieved thus far in creating the required type of beam. However, the technique has proved to be very useful in the study of phenomena in shock tubes. The acoustic plane waves when viewed by schlieren apparatus serve in a manner similar to interferometer fringes in evaluating the flow near the shock wave.

The second method considered by Flader called the "dual receiver normal incidence" technique utilized two receivers on a small boom and spaced about 6 inches apart streamwise. Another movable boom containing an emitter was located across the stream about 12 inches away. The emitter boom, when placed in a position such that the signals at the two receivers were of the same amplitude, had a displacement from the transverse $\mathbb{C}$ of the receivers directly proportional to the Mach number of the flow.

The low speed wind tunnel tests on this system gave very accurate indications of flow velocity and seem to have proven the feasibility of the system. In a series of high speed runs

up to about M = .6, the aerodynamic noise became a serious problem. In the higher ranges, it was not possible to detect the signal at all. It became apparent that, particularly for supersonic applications, a thorough knowledge of the levels of noise which might be encountered in wind tunnels should be investigated. The first experimental phase of this study was undertaken to supply such data.

The exact nature of this aerodynamic noise in wind tunnels is open to question. It would seem apparent that the fluctuations of pressure at the surface of a probe could be due to laminar or turbulent fluctuations within the boundary layer of the probe, or similar fluctuations in the main stream. In addition, environmental conditions such as wind tunnel powerplant noise, blade beats, duct resonance, etc. could conceivably contribute too. In the course of this investigation an attempt was made to isolate the possible sources, and this procedure will be described in detail.

It was also of interest to know whether or not such a probe as was used in this study could be made applicable to the general investigation of turbulence in high speed flow. With this in mind, surveys were made of the field of flow under various conditions, and these experiments are also described.

It also became apparent that, if a wide range of velocities was to be covered by a sonic airspeed indicator, a very powerful sound generator would be needed, and it would be preferable if the frequency of emission was well above the human hearing range. The types of ultra-audio transducers which have been studied for such applications include piezo-electric crystals, magnetostrictive rods, spark gaps, sirens, and whistles. The first two techniques are very useful for underwater applications, but they are hampered by poor impedance matching for use in air. However the Flader organization at this time is continuing to study the use of quartz crystal sources. Sparks are objectionable in the presence of any other electronic equipment. Air driven generators offer many possibilities. Because of its inherent simplicity, the Hartmann whistle was used in this study, and with a reasonable amount of success.

The analytical approach to the problem of determining the sound field in a moving fluid used by both Harvard and Flader was essentially ray acoustics. Their method assumed that the lines normal to the wave fronts in a stationary fluid would be displaced evenly downstream under the influence of the relative fluid motion. There was ordinarily no distinction made between the velocity rays and the pressure rays. The experimental

data available at low speeds seemed to bear out the usefulness of this method. However there was reason to believe that the method would not give a sufficiently accurate description of the sound field in higher velocity ranges. With this in mind, an approach to this problem utilizing the Lorentz and Galilean transformations was used in this study.

II. DISCUSSION OF THE ACOUSTICAL POTENTIAL EQUATIONS

The differential equation for the propagation of infinitesimal disturbances in a quiescent compressible fluid is given by the standard wave equation which can be written in the form:

$$\nabla^2 \phi_o - \frac{1}{c^2} \phi_{o\,t_1 t_1} = 0 \tag{1}$$

This has the general solution: $\phi = \frac{1}{r_1} f(t_1 + \frac{r_1}{c}) + \frac{1}{r_1} g(t_1 - \frac{r_1}{c})$ where r_1 is the radial distance to the point. However, if it is desirable to consider a relative motion between the wave source and the fluid, when a Cartesian coordinate system with the velocity parallel to the positive x-axis is used, the differential equation becomes:

$$\left\{ \nabla^2 - \frac{1}{c^2} \left[\partial/\partial t + U \partial/\partial x \right]^2 \right\} \phi_o = 0 \tag{2}$$

A. Application of the Lorentz-Galilean Transformation.

If the following transformation is applied:

$$X_1 = x/m \quad , \quad t_1 = m t + \frac{Mx}{mc}$$

where M = Mach No.

and $m^2 = 1 - M^2$

equation (2) acquires a form identical to equation (1), and

$$\phi_o = \frac{1}{r} f(mt + \frac{Mx}{mc} \pm \frac{r}{c}) \tag{3}$$

satisfies the proper differential equation where $r^2=\left(\frac{x}{m}\right)^2+y^2+z^2$. By this procedure it is readily possible to transform all solutions which satisfy the wave equation to the case which is of interest in this study. If we consider the velocity potential of a point source with harmonic time dependence and transform to the case for subsonic flow where $f(t_1+\frac{r_1}{c})=0$, since there are no "converging" waves, we can write

$$\phi_o \sim \frac{1}{r} \exp \frac{i\omega}{m}\left(mt+\frac{Mx}{mc}-\frac{r}{c}\right) \tag{4}$$

where ω is the frequency in radians/unit time. It has been shown in Reference 6 that if the source is considered to be distributed over an infinitesimal area, this satisfies the boundary conditions that $\partial\phi_o/\partial z=0$ everywhere except on this small area where it has harmonic time dependence and that the velocity amplitude there is directly proportional to the source strength.

B. The Point Source in Subsonic Flow.

If the effects of emitter size are neglected, the expression (3) corresponds to the sound field for a piezo-electric crystal oscillating normal to the z-axis in an infinite baffle, and therefore we will examine the results in detail.

If $$\phi_o \sim \frac{1}{r} \exp i\omega\left(t+\frac{Mx}{m^2c}-\frac{r}{mc}\right) \tag{5}$$

it can be seen that the surfaces of constant velocity potential amplitude at a given time are along r = const. They are ellipsoids of revolution about the origin with the major axis along the z-axis.

The surfaces of constant phase are given by $\frac{T}{m} - \frac{Mx}{m^2} = CONST = B$ say, these are the spheres defined by

$$(x - BM)^2 + y^2 + z^2 = B^2 \tag{6}$$

whose centers are displaced downstream to $x = BM$

The pressure field is defined by the condensation s, where $s = \frac{P_\infty - P}{P_0}$ and $s = \frac{\partial \phi_0}{\partial t} + U \frac{\partial \phi_0}{\partial x}$

$$\therefore s = \phi_0 \left[\frac{i\omega}{m^2} \left(1 - \frac{Mx}{mr} \right) - \frac{Ux}{m^2 r^2} \right] \tag{7}$$

If

$$W^2 = \frac{\omega^2}{m^4} \left(1 - \frac{Mx}{mr} \right)^2 + \frac{U^2 x^2}{m^4 r^4} \tag{8}$$

and

$$\delta = \tan^{-1} \frac{\omega r^2}{Ux} \left(1 - \frac{Mx}{mr} \right) \tag{9}$$

the surfaces of constant pressure phase are at $\frac{Mx}{mc} - \frac{r}{c} + \frac{\delta m}{W} = \text{const.}$ and the surfaces of constant pressure amplitude are at

$$\frac{W^2}{r^2} = \text{const} = D^2 \text{ say}$$

This can be expressed in the form:

$$x^2 \left[\frac{\omega^2 M^2}{m^2 r^2} + \frac{U^2}{r^4} \right] - 2x \left[\frac{\omega^2 M}{mr} \right] + \omega^2 - D^2 r^2 m^4 = 0$$

if $\frac{\omega^2 M^2}{m^2 r^2} >> \frac{u^2}{r^4}$, $X \doteq \frac{mr}{M}\left[1 \mp \frac{D m^2 r}{\omega}\right]$

or $$r - \frac{MX}{m} = \pm \frac{D r^2 m^2}{\omega} \qquad (11)$$

i.e. the envelope of the intersecting curves of the displaced spheres with the corresponding ellipsoids form the surfaces of constant pressure amplitude.

At $Y=0$ if $\frac{Dr m^2}{\omega} >> 1$, $X = \frac{D m^3 r^2}{M\omega} = \frac{1}{2K}(X^2 + m z^2)$

where $K = \frac{M\omega}{2DM}$ and $$(X-K)^2 + m^2 z^2 = K^2 \qquad (12)$$

These are ellipses displaced downstream so that the centers are at $X = K$. Therefore, if the contingencies mentioned are satisfied, it would appear to be feasible to measure the Mach number of a flow by detecting this center. The method used by Flader, although it was not based on this type of analysis, apparently has done this. If, in addition, the transit times of the acoustical waves to the receivers can be determined, the two parameters are sufficient to ascertain the velocity, Mach number, and the temperature of the flow.

C. The Point Source in Supersonic Flow.

Using an analysis similar to the preceding one, except that

both $f\left(t_1+\frac{r_1}{c}\right)$ and $f\left(t_1-\frac{r_1}{c}\right)$ are retained, the velocity potential for an oscillating point source is given by

$$\phi_o \sim \frac{1}{r} \cos Kr \exp i\omega\left(t-\frac{Mx}{\beta^2 c}\right) \tag{13}$$

where $\beta^2=M^2-1$, $K=\frac{\omega}{\beta^2 c}$

and $r^2=x^2-\beta^2(y^2+z^2)$

The surfaces of constant velocity potential amplitude are along r = const. These are hyperboloids of revolution, and r = 0 is the Mach cone.

The surfaces of constant phase at a given time are the circle planes bordered by the Mach cone where x = const., since

$$S=\frac{\partial \phi_o}{\partial t}+\frac{u\,\partial \phi_o}{\partial x}=-\phi_o\left[iKc+\frac{Mcx}{r}\left(\frac{1}{r}+K\tan Kr\right)\right] \tag{14}$$

The lines of constant phase are now shifted by δ where

$$\delta=\tan^{-1}\frac{Kcr^2}{Mcx\,(1+Kr\tan Kr)} \tag{15}$$

along $r=0$, $\delta=0$

If the edge of the Mach cone from a point source and the transit time could be detected it would again seem feasible to measure the Mach number, velocity, and temperature in supersonic flow. Another approach which is being investigated[7] is to make the

emitter characteristics sufficiently directional so that the $f\left(t_1+\frac{r_1}{c}\right)$ will have negligible influence on the receiver. If this is done, the subsonic analysis would, with the proper restrictions, be applicable in the supersonic range.

D. The Finite Emitter Problem

In order to get sufficiently directional properties in an acoustical emitter it is in general necessary to have the surface dimensions at least of the same order as the wave length of the signal. In principle, the potential problem can be solved by superimposing the potentials for a distribution of point sources so that if the sources are in the $\xi\eta$ – plane where $z=0$

$$\phi = \iint_S A(\xi,\eta)\phi_0(x-\xi, y-\eta, z, t)\,d\xi\,d\eta \tag{16}$$

and the boundary conditions are $\lim_{z\to 0} \frac{\partial\phi}{\partial z} \sim A(\xi,\eta)$

One particular case which appears worthy of study is the circular plate of radius a in an infinite baffle in subsonic flow. Th velocity potential can then be expressed in the following form:

$$\phi \sim \text{EXP}\, i\omega\left(t+\frac{Mx}{m^2c}\right) \int_0^a\int_0^{2\pi} \frac{1}{r}\,\text{EXP}-ik\left(\frac{M\xi}{m}+r\right)\rho\,d\rho\,d\phi$$

where $r^2 = \frac{(x-\xi)^2}{m^2} + (x-\eta)^2 + z^2$

$$K = \omega/mc$$

$$\xi = \rho\cos\psi$$

$$\eta = \rho\,\text{SIN}\,\psi$$

If the case for large values of r is considered neglecting $O\left(\frac{\xi^2}{R^2}, \frac{\eta^2}{R^2}\right)$

in the center plane where $y=0$

$$r^2 = R^2 - \frac{2X\xi}{m^2} \qquad \text{where } R^2 = \left(\frac{X}{m}\right)^2 + z^2$$

and keeping only the first two terms of the series expansion

$$r \doteq R\left(1 - \frac{X\xi}{m^2R^2}\right) \qquad \text{and} \quad \frac{1}{r} \doteq \frac{1}{R}\left(1 + \frac{X\xi}{m^2R^2}\right)$$

the area integral becomes

$$\frac{e^{-ikR}}{R}\int_0^a\int_0^{2\pi}\left(1+\frac{X\xi}{m^2R^2}\right)e^{\frac{ik}{m}\left(\frac{X}{Rm}-M\right)\xi}\rho\,d\rho\,d\psi = \frac{e^{-ikR}}{R}\left[I_1 + I_2\right]$$

where

$$I_1 = \int_0^a\int_0^{2\pi} e^{id\rho\cos\psi}\rho\,d\rho\,d\psi = 2\pi a^2\frac{J_1(da)}{da}$$

$$\text{IF} \quad d = \frac{k}{m}\left(\frac{X}{Rm} - M\right)$$

and

$$I_2 = \left(\frac{X}{m^2R^2}\right)\int_0^a\int_0^{2\pi}\rho^2\cos\psi\, e^{id\rho\cos\psi}\,d\rho\,d\psi = \frac{2\pi i X a^2 J_2(da)}{m^2R^2d}$$

Hence, the potential becomes

$$\phi \sim \frac{2\pi a^2}{R}\left[\frac{J_1(da)}{da} + \frac{iX}{dm^2R^2}J_2(da)\right]\exp i\omega\left(t + \frac{Mx}{m^2c} - \frac{R}{mc}\right)$$

If $da = \Theta$ the potential is given by:

$$\phi \sim \frac{2\pi a^2}{R}\left[\frac{J_1(\Theta)}{\Theta} + \frac{iX}{\beta m^2 R^2} J_2(\Theta)\right] e^{i\omega\left(t + \frac{MX}{mc} - \frac{R}{mc}\right)} \quad (18)$$

If $O(R^{-3})$ are neglected

$$\phi \sim \frac{2\pi a^2}{R}\left[\frac{J_1(\Theta)}{\Theta}\right] e^{i\omega\left(t + \frac{MX}{m^2 C} - \frac{R}{mc}\right)} \quad (19)$$

and

$$S = \phi\left[\frac{i\omega}{m^2}\left(1 - \frac{MX}{mR}\right) + \frac{U}{m^2 R}\left\{\frac{X}{R} + Ka\frac{J_2(\Theta)}{J_1(\Theta)}\left(1 - \frac{X^2}{m^2 R^2}\right)\right\}\right] \quad (20)$$

As before if

$$W^2 = \frac{\omega^2}{\beta^4}\left(1 - \frac{MX}{mR}\right)^2 + \frac{U^2}{\beta^4 R^2}\left\{\frac{X}{R} + Ka\frac{J_2(\Theta)}{J_1(\Theta)}\left(1 - \frac{X^2}{m^2 R^2}\right)\right\}^2$$

the lines of constant pressure amplitude are given by

$$\frac{W^2 J_1^2(\Theta)}{R^2 \Theta^2} = \text{const} = D^2 \text{ say}$$

and for large values of R this reduces to:

$$X = \frac{D\beta^3 R^2}{\omega M}\left[\frac{\Theta}{J_1(\Theta)}\right] \quad (21)$$

since $\Theta = \frac{Ka}{m}\left(\frac{X}{mr} - M\right)$ and $Ka \sim \frac{a}{\lambda}$ where λ is the wave length of the signal, as $Ka \to 0$, this reduces to the same form as the point source solution.

E. The Finite Emitter in Supersonic Flow

The velocity potential for a finite emitter in this case is given by

$$\phi \sim \exp i\omega\left(\frac{t-Mx}{\beta^2 c}\right)\iint_S \frac{\cos Kr}{r}\exp iK\frac{M\xi}{\beta}\,d\xi\,d\eta \qquad (22)$$

where S is the area of the emitter in the domain of dependence of the point (X,Y,Z)

If we again study the circular emitter in the plane of symmetry but now for large enough values of r so that the entire emitter surface is in the domain of dependence of the point, making the same approximations as before the area integral becomes

$$\frac{\pi a^2}{R}\left\{\left[\frac{J_1(d_1 a)}{d_1 a}+\frac{ix}{d_1 R^2}J_2(d_1 a)\right]e^{iKR}+\left[\frac{J_1(d_2 a)}{d_2 a}+\frac{ix}{d_2 R^2}J_2(d_2 a)\right]e^{-iKR}\right. \qquad (23)$$

where $d_1 = K\left(\frac{M}{\beta}-\frac{x}{R}\right)$ and $d_2 = K\left(\frac{M}{\beta}+\frac{x}{R}\right)$ and $R^2 = x^2-\beta^2 z^2$

if $O(R^{-3})$ are again neglected

$$\phi \sim \frac{\pi a^2}{R}\left[\frac{J_1(d_1 a)}{d_1 a}e^{iKR}+\frac{J_1(d_2 a)}{d_2 a}e^{-iKR}\right]e^{i\omega\left(t-\frac{Mx}{\beta^2 c}\right)} \qquad (24)$$

IF $\phi = \phi_1(d_1)+\phi_2(d_2)$

the condensation becomes:

$$S = \phi\left[EK\beta^2 C\left[+U\left\{\frac{x^2}{R}\left(iK-\frac{1}{R}\right)-\left\{iKM\right\}\right]-\frac{1}{R}\frac{Ka}{R}U\left[\phi\left(\frac{x^2}{R^2}-1\right)\frac{J_2(d_1 a)}{J_1(d_1 a)}+\phi_2\left(\frac{x^2}{R^2}+1\right)\frac{J_2(d_2 a)}{J_1(d_2 a)}\right]\right. \qquad (25)$$

F. The Two Dimensional Emitter in Supersonic Flow

Garrick and Rubinow[11] have considered similar problems, and by using a slightly different transformation derive the general expression for the potential at a point due to a semi-infinite emitter in the $\xi\eta$ plane whose leading edge is on the y-axis. For the case of an emitter with the surface points in phase executing harmonic time dependent vertical motion their expression becomes:

$$\phi(x,y,z,t) \sim \int_0^{\xi_1} \int_{\eta_1}^{\eta_2} \frac{e^{i\omega(t-\tau_1)} + e^{i\omega(t-\tau_2)}}{\sqrt{(\eta-\eta_1)(\eta_2-\eta)}} \, d\xi \, d\eta \qquad (26)$$

where

$$\eta_{1,2} = y \mp \eta_0 \qquad \tau_{1,2} = \frac{M(x-\xi)}{\beta^2 c} \pm \frac{r}{c}$$

$$\eta_0 = \sqrt{\frac{(x-\xi)^2}{\beta^2} - z^2} \qquad r = \sqrt{\frac{(x-\xi)^2}{\beta^2} - (y-\eta)^2 - z^2}$$

$$\xi_1 = x - \beta z$$

using the substitution: $2\eta = (\eta_2 - \eta_1)\cos\theta + (\eta_2 + \eta_1)$

the integral becomes:

$$e^{i\omega t} \int_0^{\xi_1} e^{-\frac{i\omega M}{\beta^2 c}(x-\xi)} \int_0^{\pi} \cos\left(\frac{\omega}{\beta c}\eta_0 \sin\theta\right) d\theta \, d\xi$$

or $$e^{i\omega t} \int_0^{\xi_1} e^{-\frac{i\omega M}{\beta^2 c}(x-\xi)} J_0\left(\frac{\omega}{\beta c}\eta_0\right) d\xi$$

Near the leading edge Mach wedge $J_0\left(\eta_0 \frac{\omega}{\beta c}\right) \doteq 1$

then $$\phi \sim \frac{i}{K} e^{i\omega\left(t - \frac{Mx}{\beta^2 c}\right)} \left[e^{-iK(x-\beta z)} - 1\right] \qquad (27)$$

WHERE $K = \frac{\omega M}{\beta^2 c}$

For emitters having sections of their leading edges which are essentially normal to the direction of the flow, the potential in the regions near the Mach cones emanating from this edge will be described by the above equation.

III. EXPERIMENTAL PROGRAM

A. Description of Test Equipment.

1. The Massa sound probe (Model NoGA-1005) (Fig. 1). This is a pressure sensitive device utilizing the piezo-electric properties of a 1/16" cubic APN crystal. Because of the small crystal size, this particular model has a range of frequencies from 100 cycles/sec. to 250 kilocycles/sec. It was designed to measure amplitudes up to one atmosphere linearly.

The crystal itself is mounted in a fairly solid plastic material with the sensing face cemented to a very thin metal diaphragm. The whole sensing element is in the form of a metal bound cylinder 5/8" long and with an outside diameter of .135". The electrode plates of the crystal are electrically connected by means of a rigid low capacity coaxial cable approximately 3" long to a cathode follower preamplifier. This configuration minimizes the attenuation and pick-up noise which plagues all such devices.

2. Wave Analysis Equipment.

For these experiments, the signal from the Massa probe, after it left the preamplifier, was fed directly to the antenna posts of a U.S. Navy RAK-5 radio receiver which was used as an amplifier-filter for wave analysis. This is a TRF unit, and has a frequency range from 15 KC to 600 KC. In this particular application, only the first three stages of amplification were utilized.

The amplified signal was fed into a Ballantine vacuum tube voltmeter, and thereby the mean signal amplitudes were recorded.

3. Wind Tunnels

The 2 1/2" C.I.T. Supersonic Wind Tunnel.

The general description of this tunnel is given in Ref. (12). In these tests, a set of two dimensional wooden nozzle blocks, designed for Mach numbers of .98, 1.4, 2.0, and 2.68, were used. For the static pressure runs, each of the blocks was modified to accommodate a small adapter so that the sensitive face of the probe would lie as close to the surface of the test section as possible. The adapters had a .002" lip which retained the sensing head without touching the pressure sensitive region.

The C.I.T. Hypersonic Wind Tunnel

A general description of this installation is given in Ref. (13). For the tests run in connection with this study, the hole through which the model supports usually run were modified with adapters similar to those described above to accommodate the Massa probe.

4. The Flat Plate Model. (Fig. 2)

This model was designed to simulate conditions in a boundary layer at relatively low Reynolds numbers. All frontal dimensions were minimized to prevent blockage. It was possible to vary the angle of attack through fairly wide ranges, and later on it was arranged so that the whole assembly could be moved horizontally

during test runs (fig. 3). The microphone could be placed either 3/4" or 2" from the leading edge, very nearly flush with the surface.

5. The Total Pressure Stand. (Fig. 2)

This consisted of a brass tube with an O.D. of .25". The tube was mounted at right angles to a hollow biconvex section, and a 6" coaxial cable ran through the center of the stand to conduct the signal to the preamplifier unit. The cable was calibrated, and it caused a constant attenuation of 50 db over the frequency range considered. The whole unit was so mounted that both vertical and horizontal traverses of the test section center plane could be accomplished.

6. The Hartmann Ultra-Audio Sound Generator. (Fig. 3)

This type of system was chosen for the sound propagation experiments because of its inherent simplicity, and availability. It is essentially a whistle which works on the basis of an air jet impinging on a resonant cavity. It is particularly useful in the higher frequency ranges where mechanical devices cannot be excited to resonance. The particular device which was used in this work was a modification of the Hartmann design so that higher pressure ratios could be utilized.

In his original works [8] Hartmann was unable to specifically explain the mechanics of his device, but he noted that a

pressure ratio greater than that corresponding to an isentropic expansion of the fluid to Mach one was required to bring the whistle into operation. He also examined the jet pattern with schlieren apparatus and noted that if the pressure ratio was increased beyond a certain point, "breakdown" of the signal resulted. Hartmann found that as the distance between the orifice and the chamber was varied there were alternate regions where a signal was, and then was not, produced. The author, following a rather heuristic approach, offers the following explanation of the operation of this system:

As the air leaves the orifice it takes on a characteristic pattern typical of supersonic jets exhausting into regions of lower pressure. (See Fig. 18). The boundary takes the form of alternately diverging and converging sections. As the jet impinges on the body containing the resonant chamber, a normal shock is formed. If this shock is placed in a diverging section, it will be stable, but if it is formed within a converging section it has been shown[9] that it is unstable, and will move upstream, destroying its boundary as it goes until it again reaches a diverging section. At this point, it will again move downstream to the mouth of the chamber. This process is repeated at a very high rate, and the density discontinuity of the normal shock acts as a diaphragm which, when in harmony with the chamber resonance frequency, produces

high intensity sound waves.

It was noted that the "breakdown" which Hartmann mentioned is really what is now termed "Mach reflection", i.e. the jet pattern becomes so steep that the compression can only be accomplished by a process which includes a normal shock in part of the region. Such a shock will have a subsonic field behind it which will destroy the pattern.

In order to increase the output of such a whistle it is desirable to have the following two conditions existant:

1. A steep density discontinuity through the normal shock "diaphragm"
2. A long characteristic wave length to the jet pattern so that the range of oscillation of the shock can be increased.

Both conditions are satisfied by an increased Mach number of the flow from the orifice.

In this study, to accomplish this, a set of small nozzles were designed to replace the usual untapered orifice. These permitted the use of higher pressure ratios. The particular nozzle used in the wind tunnel work had an exit design Mach number of 1.5 and this installation had almost twice the intensity of a simple orifice whistle. This unit was contained within a 1/2" diameter

brass tube, which was cut out at the middle to permit propagation normal to its axis.

For the wind tunnel work, the unit was submerged within the nozzle block so that the sound was propagated into the test section through a 1/2" diameter hole. The rear end of the whistle was vented to a region of pressure lower than the test section pressure so that the air which formed the jet could be bled off with a minimum of disturbance to the main blow. Actually, it was not possible to detect the effect on the test section flow of the air that did escape.

B. Description of Experiments.

1. Calibration of Receiver Apparatus:

In determining the characteristics of the receiving equipment, the procedure was divided into the following steps:

a) frequency calibration of electronic circuit

b) amplitude calibration of electronic circuit

c) sensitivity calibration of crystal

a) The frequency calibration procedure for the RAK-5 consisted of placing a signal of known frequency from a Hewlett-Packard 200A oscillator into the unit and tuning the dial until the output voltage of the amplifier peaked. The dial reading of the receiver corresponding to each setting was noted. To obtain a high degree of accuracy, the oscillator signal was compared with the signal from a Beat Frequency oscillator by means of the Lissajou figures created on an oscilloscope screen.

b) For a fixed receiver dial setting, the frequency of the oscillator was varied over a wide band, holding the input voltage constant. The resultant gain was plotted for use in the spectral analyses.

c) Crystal calibration:

This work was done in the anechoic chamber at U.C.L.A. under the guidance of Dr. Rudnick. The technique utilized was the standard free field reciprocity procedure[9]. Two G.E. 640 AA

condenser microphones were utilized. These steps were followed in obtaining the necessary data:

(a) First, a condenser microphone, used as a sound source, was placed at a distance of 6" from the crystal microphone. A signal of known intensity and frequency was placed across the condenser microphone circuit, and the resultant output voltage obtained from the crystal circuit was recorded.

(b) This procedure was repeated with the other condenser microphone in place of the crystal microphone.

(c) The condenser microphone used as a receiver replaced the one used as an emitter, and the procedure of step 1 was repeated.

The frequency was varied in small increments from 15 KC to 200 KC, and the necessary data recorded.

The following relationship has been established for this calibration (10) P. 121:

$$M_o = 10^{-3.5} \left[\frac{E_o E_o'}{V_x E_x} \frac{10 d \Omega}{\rho c} \right]^{\frac{1}{2}}$$

where M_o is the response of the crystal in volts/micro bar

E_o is the response of the Massa crystal to signal from the non-reversed G.E. microphone

E_o' is the response of the G.E. microphone to signal from the reversed G.E. microphone

E_x is the response of the reversed G.E. microphone

V_x is the voltage across a 5 ohm resistor in the emitter circuit which measures the current flowing to the emitter

d is the distance between the two units in cm

ρ is the density of the medium

$\frac{c}{\lambda} = 2\pi\omega = f$ is the frequency of the signal in cycles/sec

The output of the Massa crystal was circuited through the Massa preamplifier and the RAK unit, while the condenser microphones used a special cathode follower circuit in addition to the RAK. To determine the actual E's and V's the gain of the respective amplifier system in decibels was subtracted off. If the gain of the RAK in decibels is denoted by G, the gain of the Massa preamplifier in decibels is denoted by H, the gain of the Cathode Follower in decibels is denoted by L, and if we denote the values in decibels by subscript (1) then

$$M_{o_1} = -19 + \frac{1}{2}\left[E_{o_1} + E_{o_1}' - V_{x_1} - E_{x_1}\right] - \frac{1}{2}\left[G_1 + K_1 + 2L_1 + f_1\right]$$

for these tests, $10 \log_{10} \frac{d}{\rho} \doteq 41$

THE RESULTANT SENSITIVITY VALUES

are plotted in figure 8.

Discussion of Calibrations.

The frequency and amplitude calibrations of the RAK-5 were conducted under well controlled conditions, and it is felt

that the results should be accurate within the limits of normal experimental error.

The reciprocity calibration of the Massa probe was somewhat less satisfying in this respect. The type of facility used did not permit any study of the effect of mean pressure variation upon the characteristics of the crystal, and in the light of the peculiar characteristics of the results obtained, such an additional calibration would be very desirable when it can be accomplished.

As can be seen from the resultant calibration curve, the crystal has dips in its response at about 32 KC and at 60 KC. A detailed study of these regions during the calibration showed that the 60 KC dip was not completely stable. Each run through this critical range gave a slightly different set of readings. This would seem to indicate that the mounting material for the crystal might be elastic enough to have a resonance point there. It is felt that the irregular character of the spectral curves measured at low ambient pressures might be attributable, at least in part, to a shift in the resonance frequency of the crystal mounting.

2. Noise Surveys

In all of the analyses of the spectra of pressure pulsations which were made in the course of this study, the following procedure was used.

a) Let $F(\omega)$ be spectral function in microbar/KC

$G(w)$ be gain of circuit as described in (2) P.23, in volts/out/volts/in

$M(w)$ be response of crystal in volts in/microbar

The system is subjected to the signal of $F(w)$ and the output of the amplifier is read with a vacuum tube voltmeter as $N(w_0)$

The pressure amplitude in an infinitesimal bandwidth dw is $F(w)dw$ and $N(w_0)=\int_0^\infty F(w)M(w)F(w)dw$ if M and F can be considered to be reasonably constant for the integration

$$N(w_0) = FM\int_0^\infty G(w)dw \qquad \text{Let } K(w_0)=\int_0^\infty G(w)dw$$

if we denote by subscript (1) the values of these parameters in db; F_1 in db from 1 microbar/KC, N_1 in db from 1 volt, M_1 in db from 1 volt/microbar, and K_1 in db from 1 KC volt out/volt in

Then $F_1=N_1-(M_1-K_1)$

K_1 was obtained by using a planimeter on the tuning curves obtained according to the method outlined on page 23 and M_1 resulted from the reciprocity calibration. N_1 was, of course, the value obtained from the Ballantine meter.

a. Static Pressure Noise Surveys at the Wall of Wind Tunnel Sections

Using the modified nozzle blades described on page 18, runs were made at various values of Mach numbers and total pressures. In each case, the value of the signal which reached the Ballantine meter was recorded as a function of the RAK dial setting. These data were reduced according to the procedure outlined above and the results are shown in figures 9-13.

To investigate the extent to which the sound waves propagating downstream through the nozzle throat would affect the signals in the test section, the probe was also mounted flush with the wall of the settling section about two feet ahead of the throat. These noises were found to be of a much lower order, and obviously not a main source of the pressure fluctuations measured.

b. Static Noise Surveys on a Flat Plate Model.

The flat plate model was placed on the lower surface of the M = 2.0 nozzle block so that the upper surface of the plate was approximately at the center line of the test section, and gave conditions there which closely approximated two dimensional flow.

Runs were made at several angles of attack, with the boundary layer over the probe varying from laminar to turbulent and the resultant spectral curves are shown in figures 14 and 15.

Although the model cross sectional area gave about one half the critical A/A^*, considerable difficulty was experienced due to blockage, particularly at high angles of attack. It was possible however to obtain a fairly clean laminar boundary layer over the probe under certain conditions (Cf. Fig. 4). The noise levels experienced under these conditions were actually higher than those obtained at the tunnel wall. In the forward position where the boundary layer was thinnest the signal was the strongest of all.

c. Total Pressure Surveys.

These runs were made using the stand described on page 19 The sensitive surface of the probe was perpendicular to the flow direction, and it was of interest to investigate the effect of various conditions in the wind tunnel upon the characteristics of the total pressure fluctuations. In making vertical surveys through the test section, it was found that the amplitude level at all frequencies increased as the wall was approached. The general level was about 50 db above the static pressure spectra.

Also, the probe was held at the axial centerline of the tunnel and a small rod was slowly inserted about 1" ahead of the probe to study the effect of introducing a turbulent wake. It was found that the level rose about 20 db when the turbulent wake reached the probe.

Finally, a cap was placed on the front end of the stand so that the normal shock produced was displaced forward. The effect of this upon the noise levels obtained was not noticeable.

3. Sound Field Measurements

Prior to seriously modifying the nozzle blocks, it seemed advisable to ascertain whether or not the equipment on hand would actually produce a signal of sufficient intensity to make measurements feasible.

To do this, the probe was again placed in the position flush

with the test section wall of the M = 2.0 block behind the Mach cone emanating from the leading edge of the whistle orifice. After considerable difficulty, a clear sinusoidal signal 20 db above the noise level was obtained at 20 KC.

Flat Plate Surveys.

Next, the block was modified to accommodate a micrometer traversing mechanism so that a detailed study could be made of the sound field in the vicinity of the Mach cone with the flat plate model.

Whereas, if the boundary layer effects were ignored, one would expect a sharp discontinuity in the signal strength as the edge of the cone was passed, the experiment showed quite a slow change at the edge. See Fig. (16). Attempts were made to alleviate this condition by placing small wires behind the probe to act as boundary layer "barriers", and also by using large negative angles of attack to thin down the boundary layer, but these met with negligible success.

Total Pressure Sound Surveys.

The total pressure stand was adapted to the traversing mechanism so that all positions in the test section vertical center plane could be reached and a complete survey was made of the sound field. The results are shown in Fig. (17).

It can be seen that the Mach line from the whistle is de-

fined within reasonable limits, and that it would appear feasible to measure the Mach number of a supersonic flow in this manner.

IV. CONCLUSIONS

1. Analytical results.

It is seen in the foregoing analysis that the method of the transformed acoustical potential is very useful in the study of sound fields in moving fluids. The results indicate the necessity for emphasizing the difference between the velocity and pressure waves, and, of course, satisfying the proper boundary conditions.

In the cases where the emitter size is small compared to the wave length, and the emitter surface exhibits an in-phase harmonic fluctuation, the measurement of velocity and temperature of a flow is theoretically possible by the use of either the velocity or the pressure potentials.

If velocity receivers such as hot wire microphones are used, the subsonic Mach number can readily be obtained by arranging two such receivers in tandem streamwise positions. Moving them to positions of equal phase will displace them downstream from the source a distance which is directly proportional to Mach number and if the phase difference between the source and the receivers is measured, the sound velocity can readily be determined, and hence temperature and velocity.

In supersonic flow, if one of the receivers is used as a probe to determine the edge of the silence zone, and the other to measure phase, the desired parameters can again be deter-

mined. If pressure receivers such as piezo-electric crystals are used, it is also possible for sufficiently large distances from the emitter to measure Mach number by displacing the two tandem receivers to a position of equal pressure amplitude, or of equal phase, and also for sufficiently small values of δ, the phase distortion parameter, to determine transit time by phase difference measurements. The supersonic case can be handled in the same manner as with the velocity receivers.

In cases where emitter size affects the sound field patterns, the problem becomes still more complex, and the simple techniques just described are not necessarily sufficient. It would seem desirable therefore to use fairly low ultra-audio frequencies, and small emitter areas in such devices. This would also be desirable to eliminate the possibility of ambiguities inherent in the higher frequency ranges due to having more than one position of equal phase for the two receivers. An alternate procedure to avoid this ambiguity would be to modulate the signal with a lower frequency component.

2. Experimental Results

The practical problems associated with such devices are considerable, but apparently not insurmountable. For supersonic wind tunnel applications, the noise levels over which the acoustical signals must be heard are quite impressive. It is seen from the accompanying graphs (Figs. 9-13) that there exist along the wall of the particular tunnel tested levels as high as 130 db above 1 μbar/KC or 204 db above the usual acoustics standard of 0.0002 μ bars. It is also seen that the noise is not "white" but has less energy in the upper frequency ranges. To compare the results at various Mach numbers, because of the variation in ambient pressures, it is desirable to normalize all of the curves through some frequency, say 15 KC. If this is done it can readily be seen that there is a definite shift of the energy distribution to higher frequencies with increasing Mach number. From the flat plate runs it can be seen that removing the probe from the turbulent boundary layer at the wall did not decrease the noise levels, but rather, the thinner and more laminar the boundary layer, the louder the noise! No attempt will be made herein to explain these phenomena, but rather, to simply report the results. Also, it must be left to flight tests in the free atmosphere to determine the extent to which noise will be a problem in aircraft application.

There is considerable work being done on the design of electronic circuits which are receptive to only an extremely narrow

band of frequencies. Since the noise level at a discrete frequency will be nil, if the receiver band can be made sufficiently narrow, noise may become an unimportant consideration.

The Hartmann whistle with the modifications described heretofore appears to be a useful tool for high frequency acoustical wave production, particularly in wind tunnel applications. Since the jet pattern is controlled by the ratio between the ambient and supply pressures, it would require rather careful, and possibly quite complex designing to make it feasible for operation in aircraft under a wide range of operating altitudes.

The acoustical field measurements in supersonic flow indicate that it is possible to locate the zone of silence with a small pressure microphone within rather narrow limits, and hence to determine the Mach number with reasonable accuracy.

The use of small piezo-electric crystals as turbulence probes in high speed flows appears to be worthy of further study. The results of this rather cursory investigation seem to show that such a probe is at least responsive to changes in turbulence levels. Of course, it is very desirable to first establish a theory of pressure fluctuations in turbulence, and then to correlate the results of a well controlled set of experiments with such a theory.

REFERENCES

1. ONRD Report No. 5369, Vols. I & II (1945)

2. Elrod, H. G., "The Propagation of Small Disturbances in Boundary Layers of Compressible Fluids", ONR TM No. 13 (NR-014-903) (1949)

3. BUAER Report No. IH-931-P-15 (1947)

4. Marlow, Neiswander, and Cady, "A Method for the Instantaneous Measurement of Velocity and Temperature in High Speed Air Flow", Physical Review, Volume 24 (1948)

5. Evvard, J. E., "A Linearized Solution of Time Dependent Velocity Potentials Near Three Dimensional Wings at Supersonic Speeds", NACA TN 1699 (1949)

6. Miles, J. C., "Aerodynamic Forces on an Oscillating Airfoil at Supersonic Speeds", J. Aero. Sciences (1947)

7. Progress Report No. 155-6, USAF Contract No. AF-339038-7880 (1950)

8. Hartmann, A., Philosophical Magazine, Vol. 13 (1931)

9. Kantrowitz, A., "Formation and Stability of Normal Shock Waves in Channel Flows", NACA TN 1225 (1947)

10. Beranek, L. L., Acoustical Measurements, pp. 113 (1949)

11. Garrick and Rubinow, "Theoretical Study of Air Forces on an Oscillating or Steady Thin Wing in a Supersonic Main Stream", NACA TN 1383 (1947)

12. Puckett and Schamberg, "Final Report-GALCIT Supersonic Wind Tunnel", GALCIT Library (1946)

13. Puckett and James, USORD Contract W-04-200, Progress Report No. 21 (1949)

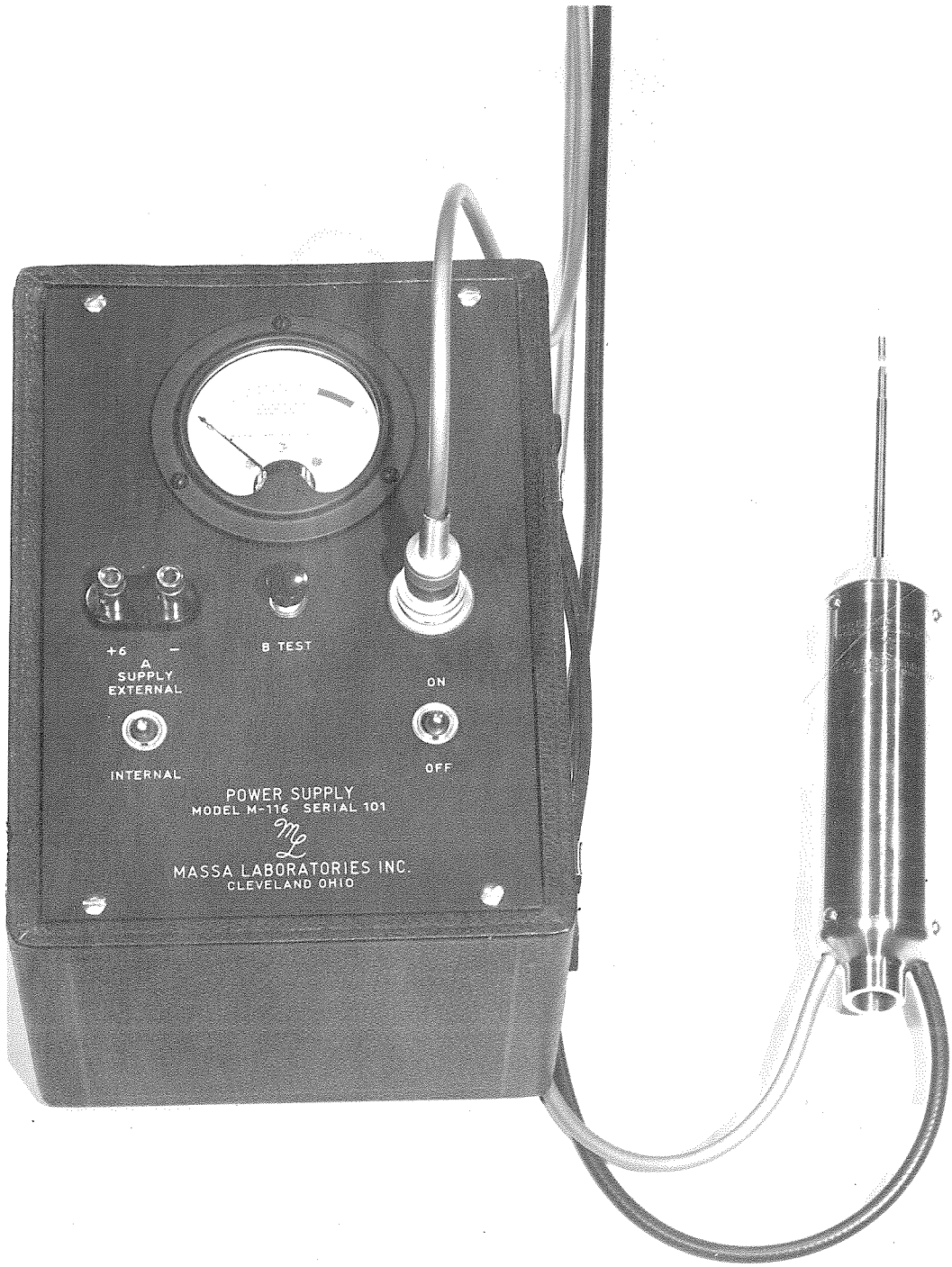

Model GA-1005 Sound Pressure Measurement System

Fig. 1

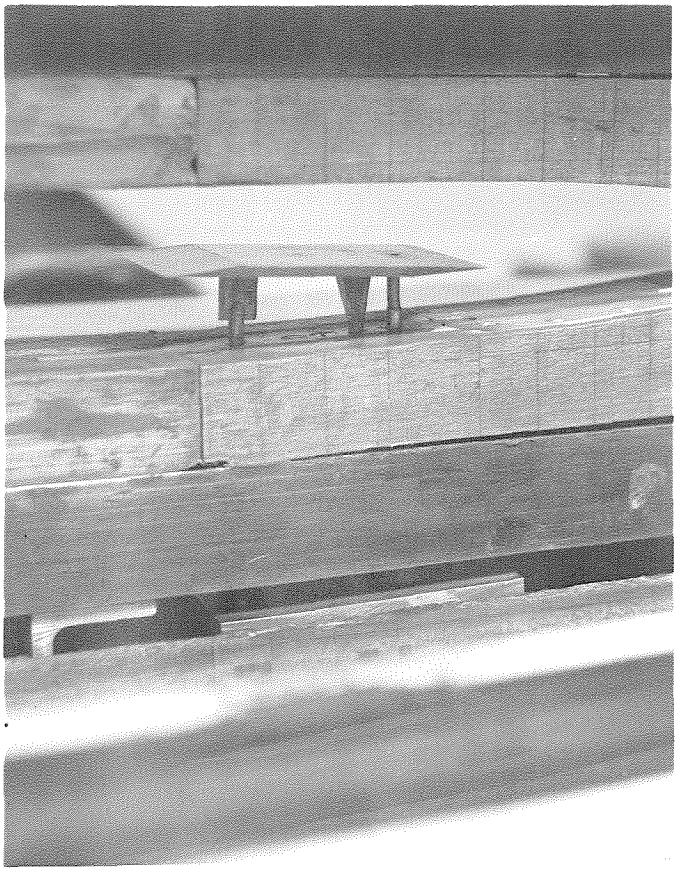

Flat plate model installed in test section.

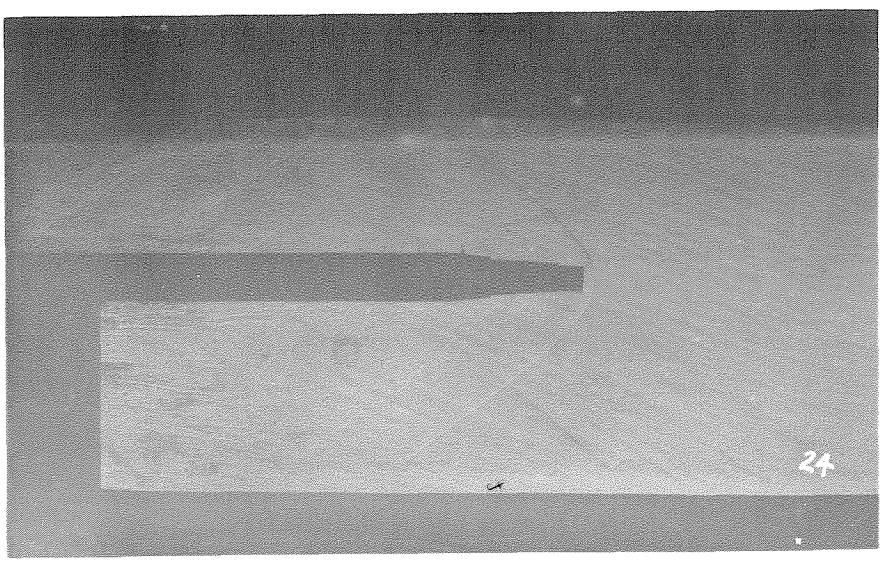

Schlieren photograph of total pressure probe.

Fig. 2

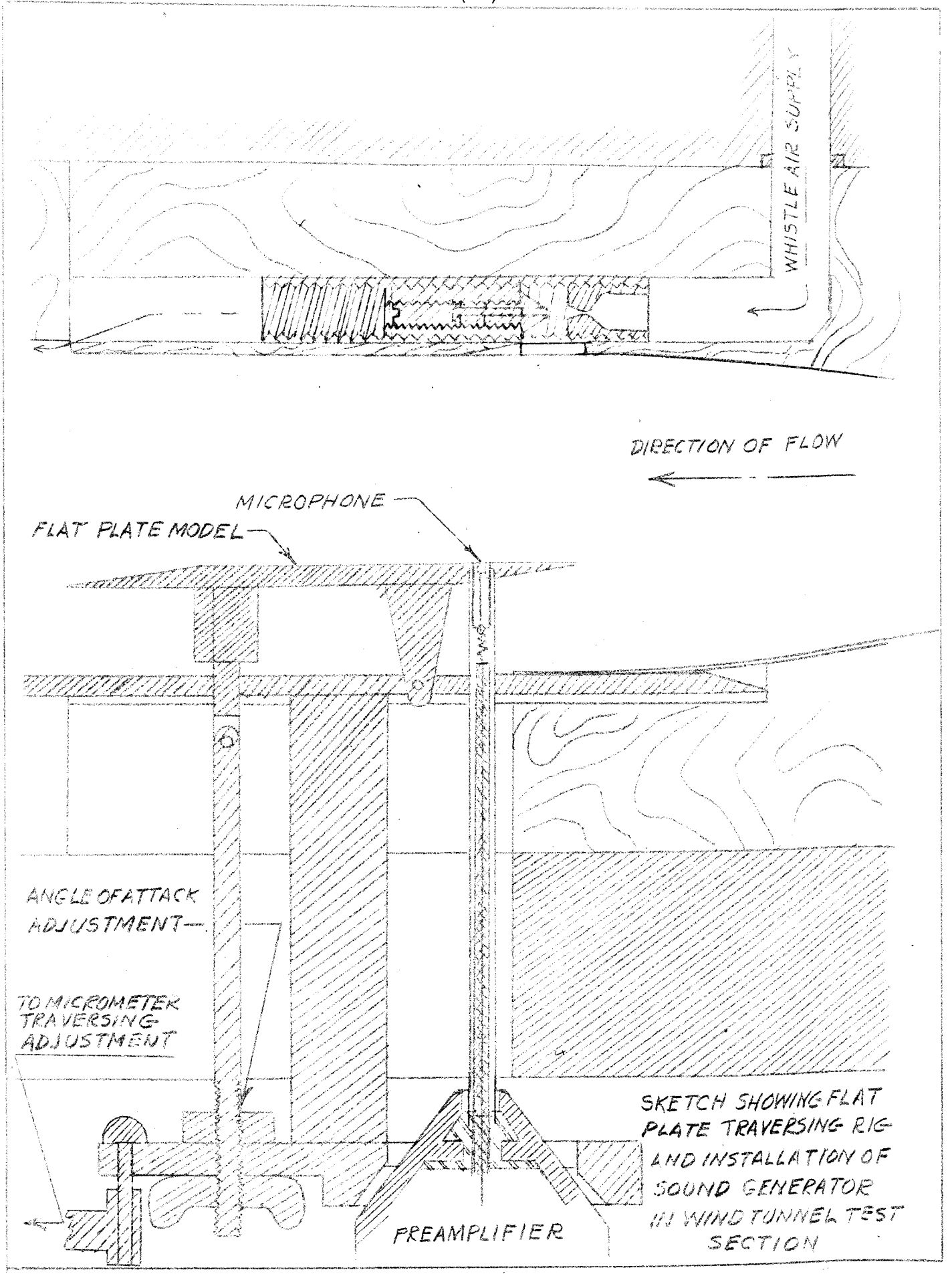
WHISTLE AIR SUPPLY
DIRECTION OF FLOW
MICROPHONE
FLAT PLATE MODEL
ANGLE OF ATTACK ADJUSTMENT
TO MICROMETER TRAVERSING ADJUSTMENT
PREAMPLIFIER
SKETCH SHOWING FLAT PLATE TRAVERSING RIG AND INSTALLATION OF SOUND GENERATOR IN WIND TUNNEL TEST SECTION

FIG 3

Schlieren photographs showing flat model with probe in rear position.

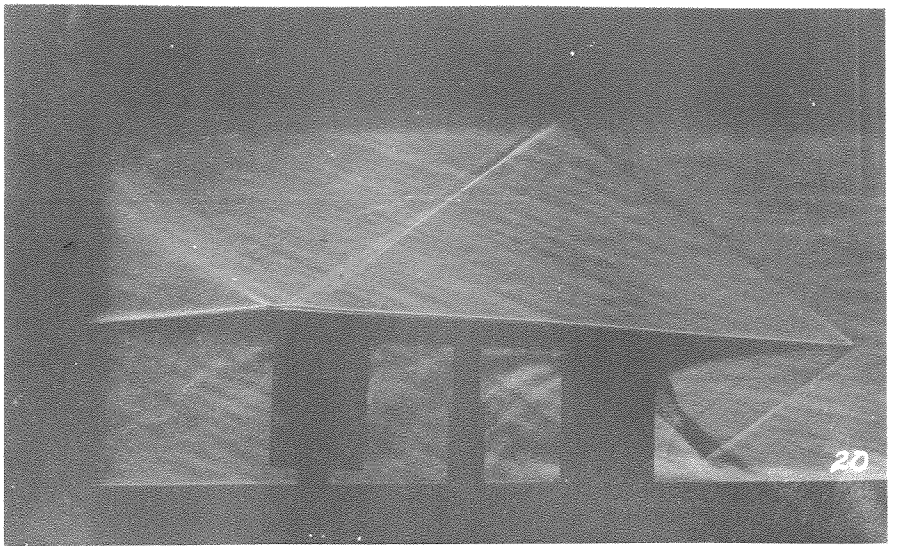

Laminar boundary layer over probe.

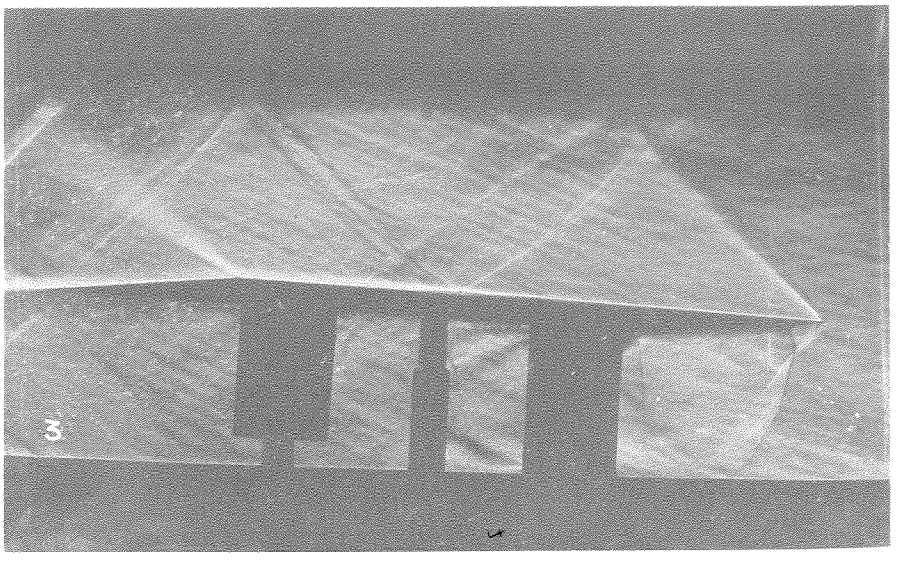

Turbulent boundary layer over probe produced by reflected shock wave.

Fig. 4

Schlieren photographs showing flat plate model with probe in forward position.

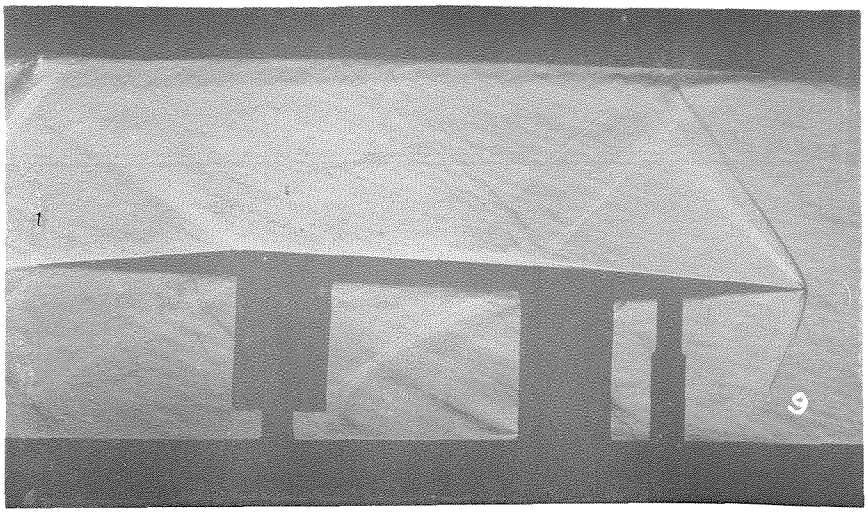

Laminar boundary layer over probe.

Turbulent boundary layer over probe produced by small wire at leading edge.

Fig. 5

Schlieren photographs showing total pressure probe.

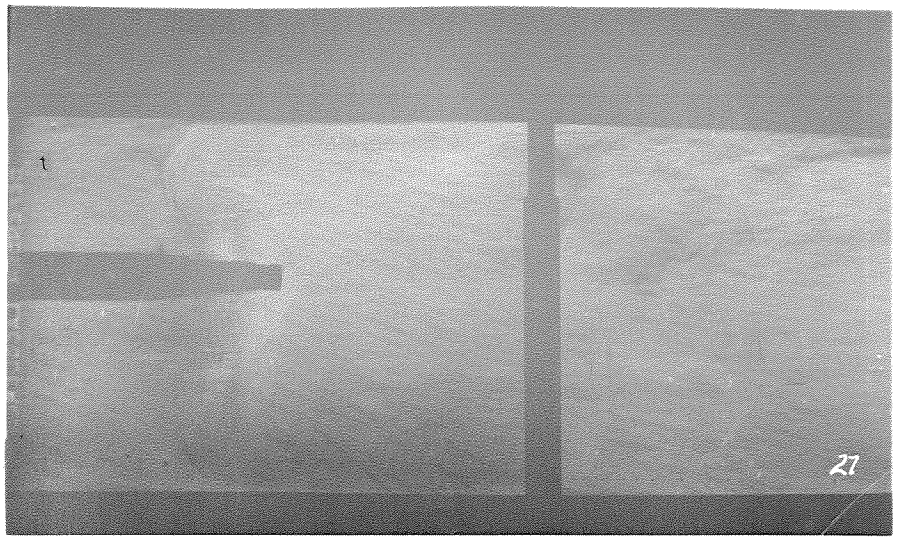

View showing flow with rod inserted ahead of probe.

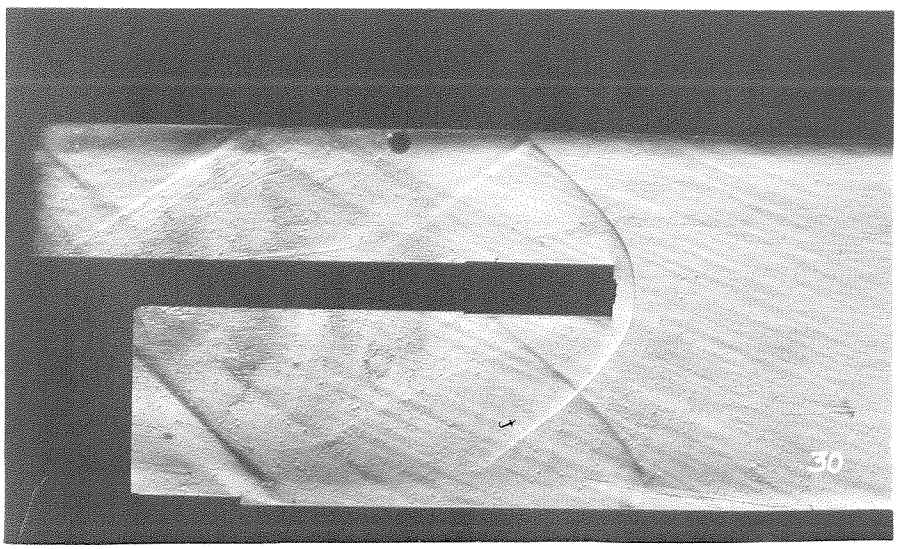

View with cap placed around microphone to displace shock.

Fig. 6

Schlieren photographs taken during sound field measurement runs.

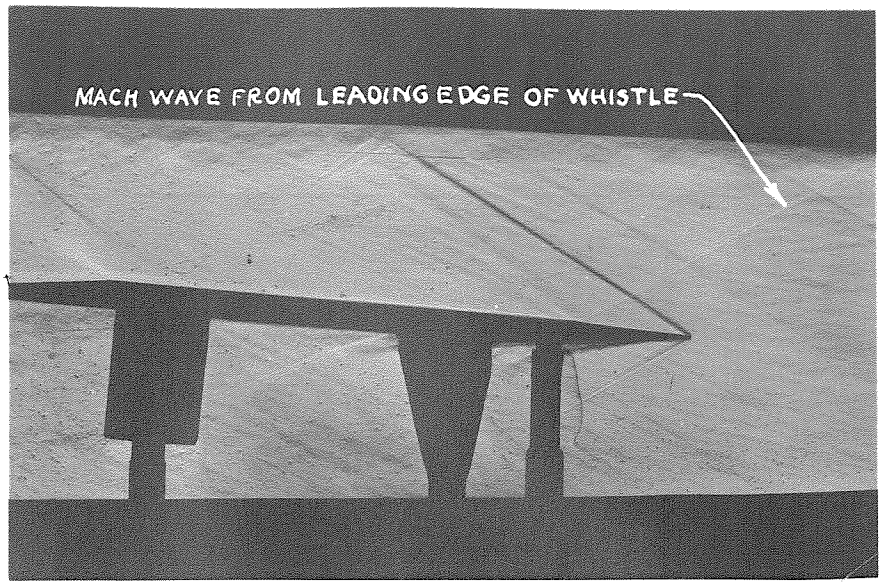

View of flat plate model.

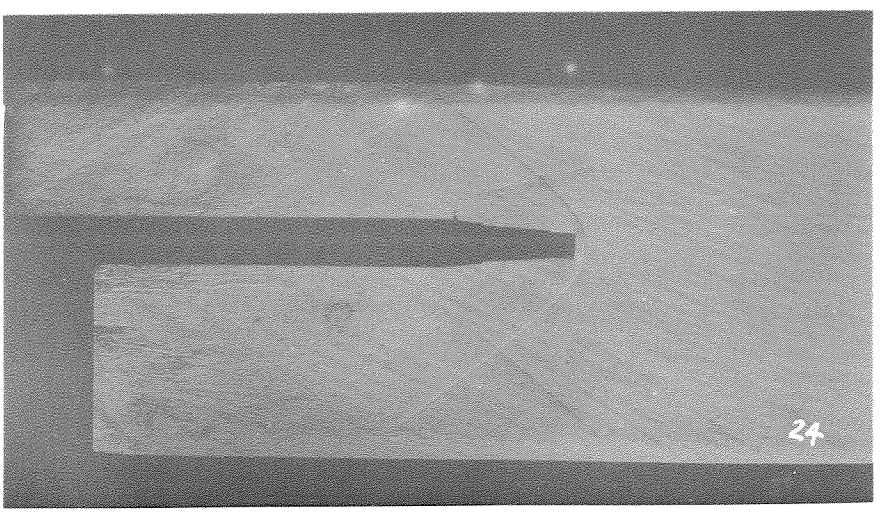

View of total pressure probe.

Fig. 7

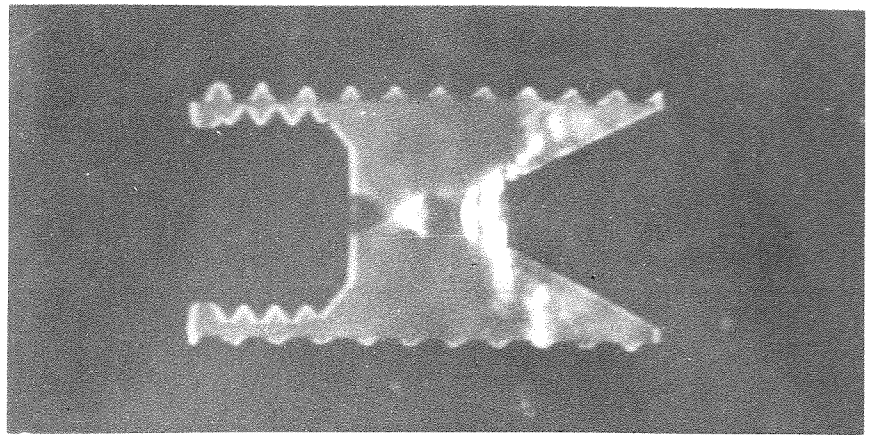

Enlarged Schlieren photograph of Hartmann Generator.

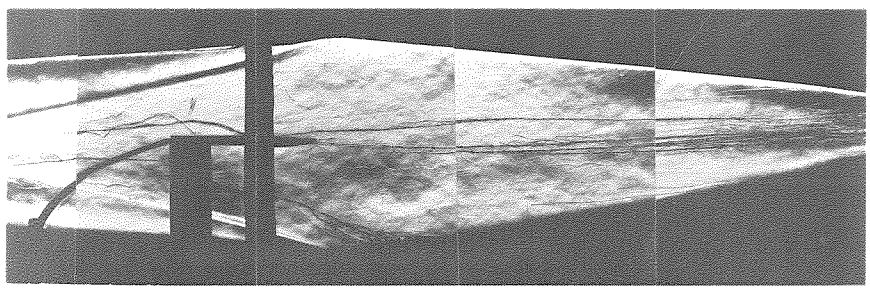

Schlieren photograph taken during noise surveys in hypersonic tunnel.

Fig. 7B

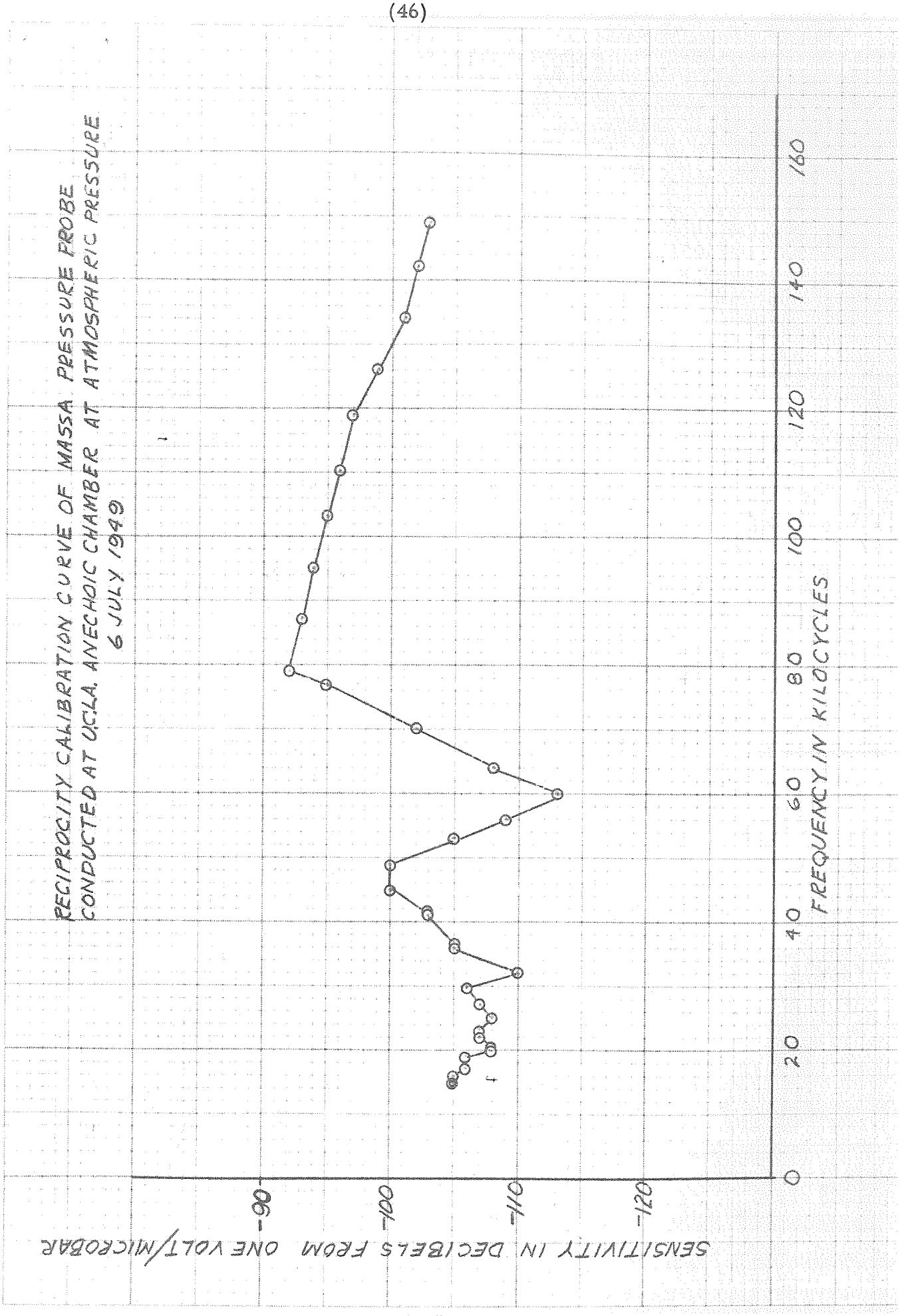
RECIPROCITY CALIBRATION CURVE OF MASA PRESSURE PROBE
CONDUCTED AT UCLA. ANECHOIC CHAMBER AT ATMOSPHERIC PRESSURE
6 JULY 1949
SENSITIVITY IN DECIBELS FROM ONE VOLT/MICROBAR
-90
-100
-110
-120
0
20
40
60
80
100
120
140
160
FREQUENCY IN KILOCYCLES

FIG. 8

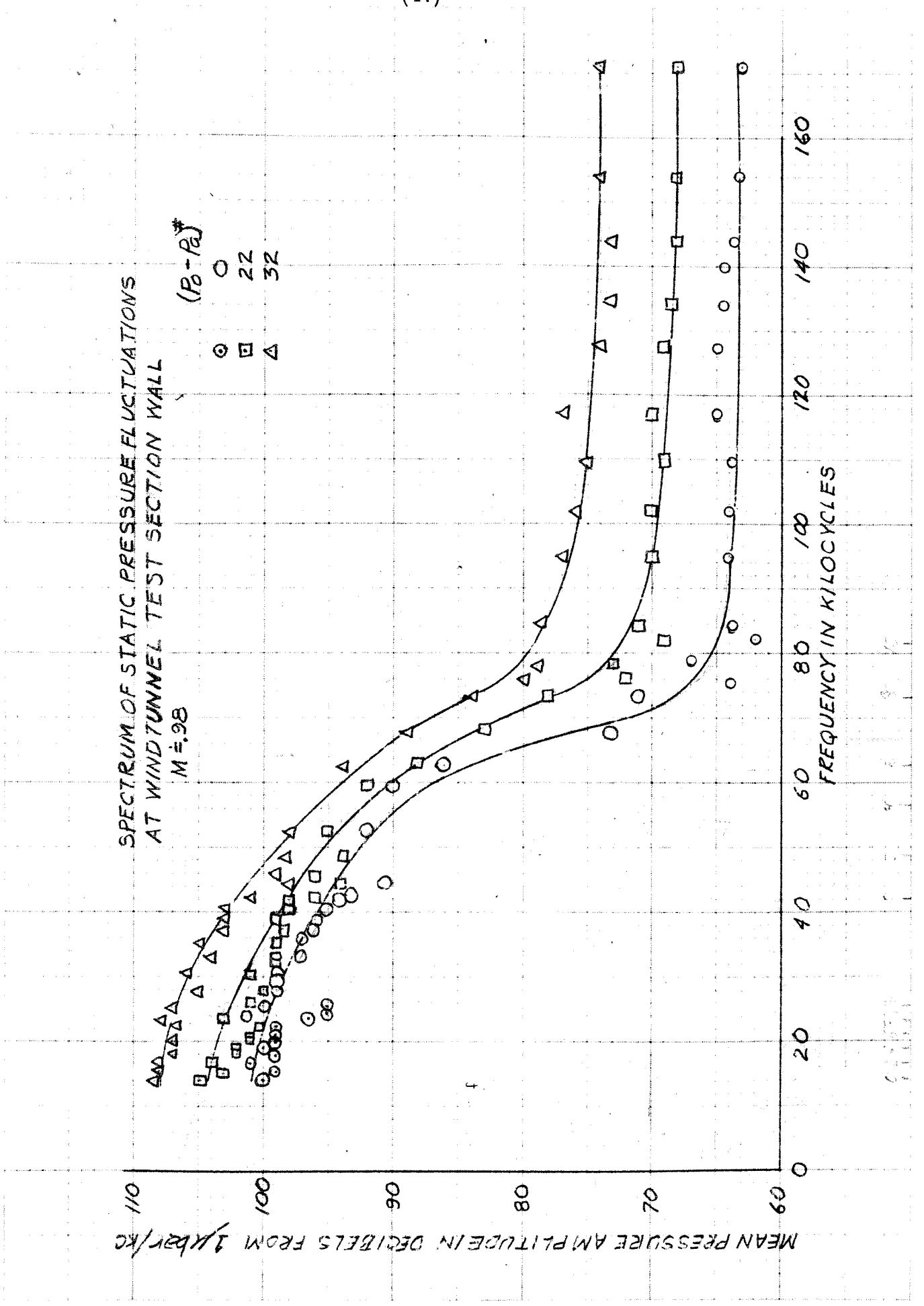
SPECTRUM OF STATIC PRESSURE FLUCTUATIONS
AT WINDTUNNEL TEST SECTION WALL
M = .98
(Pb-Pa)*
22
32
MEAN PRESSURE AMPLITUDE IN DECIBELS FROM 1 dyne/sq
110
100
90
80
70
60
0
20
40
60
80
100
120
140
160
FREQUENCY IN KILOCYCLES

FIG 9

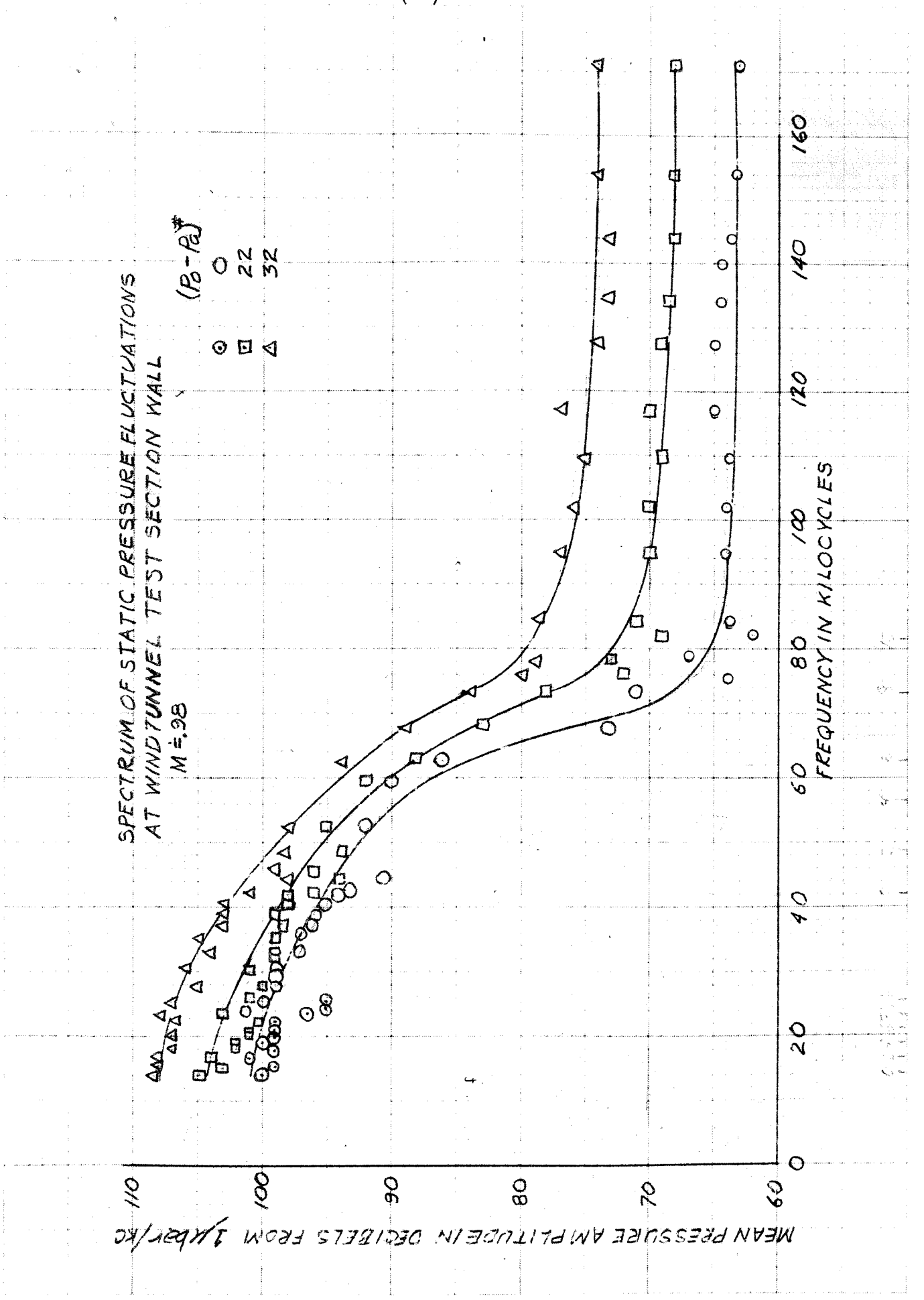
SPECTRUM OF STATIC PRESSURE FLUCTUATIONS
AT WINDTUNNEL TEST SECTION WALL
M = .98
$(P_0 - P_2)^*$
22
32
MEAN PRESSURE AMPLITUDE IN DECIBELS FROM 1 Mbar/sq
110
100
90
80
70
60
0
20
40
60
80
100
120
140
160
FREQUENCY IN KILOCYCLES

FIG 9

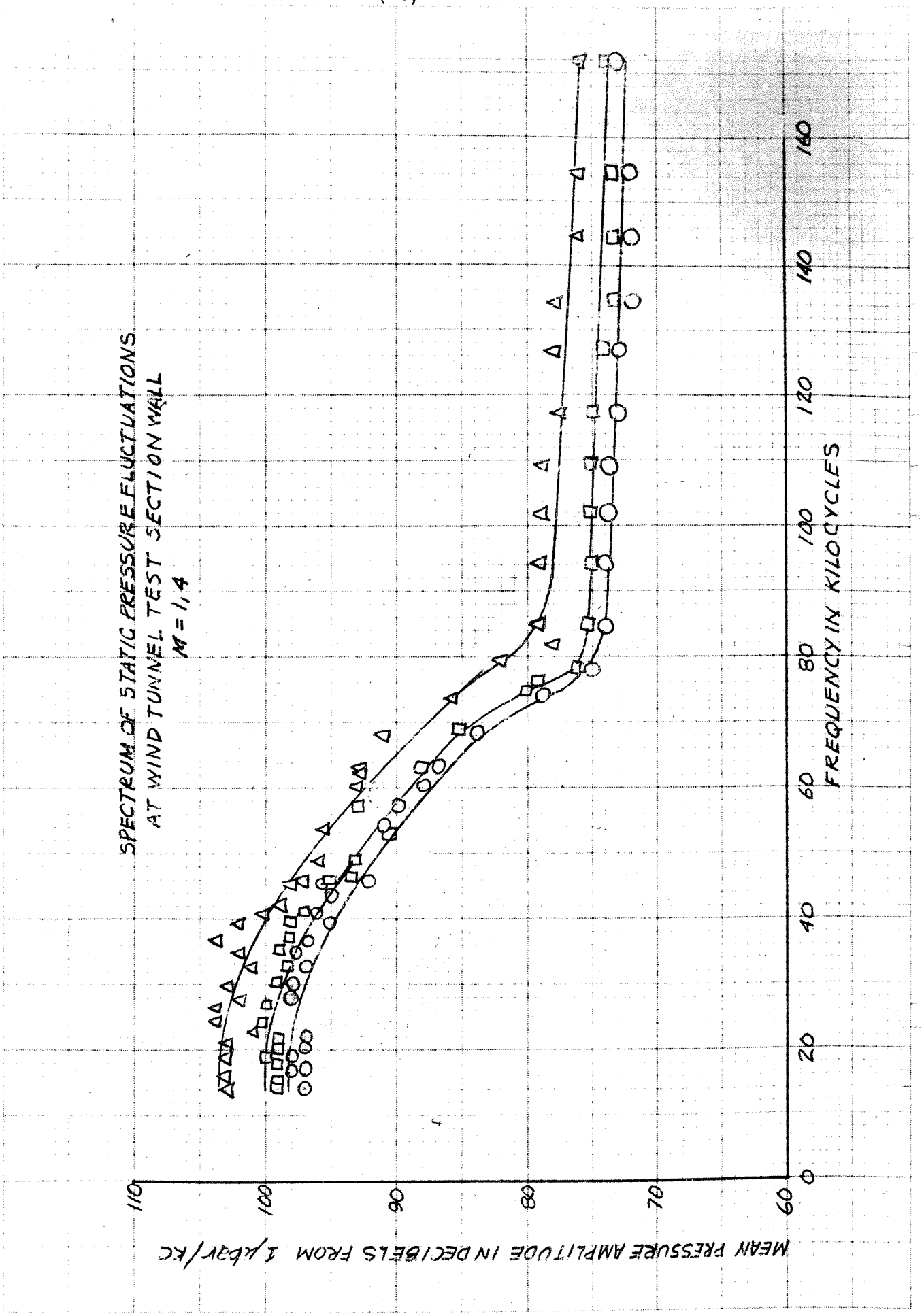
SPECTRUM OF STATIC PRESSURE FLUCTUATIONS
AT WIND TUNNEL TEST SECTION WALL
M = 1,4
MEAN PRESSURE AMPLITUDE IN DECIBELS FROM 1 Kbar/KC
110
100
90
80
70
60
0
20
40
60
80
100
120
140
160
FREQUENCY IN KILOCYCLES

FIG 10

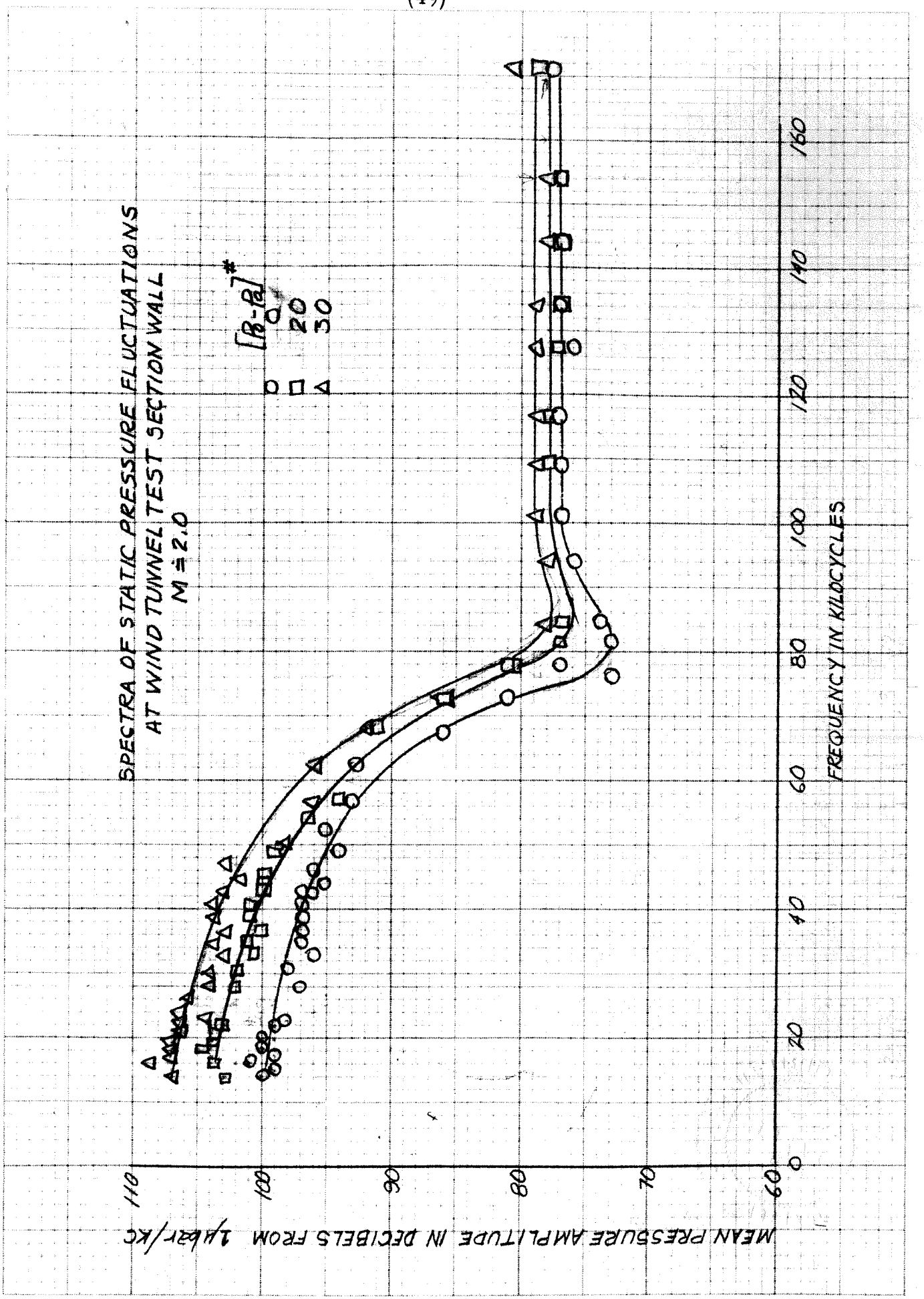
SPECTRA OF STATIC PRESSURE FLUCTUATIONS
AT WIND TUNNEL TEST SECTION WALL
M ≐ 2.0
[B-2]*
0
20
30
MEAN PRESSURE AMPLITUDE IN DECIBELS FROM 1 μbar/KC
110
100
90
80
70
60
0
20
40
60
80
100
120
140
160
FREQUENCY IN KILOCYCLES

FIG 11

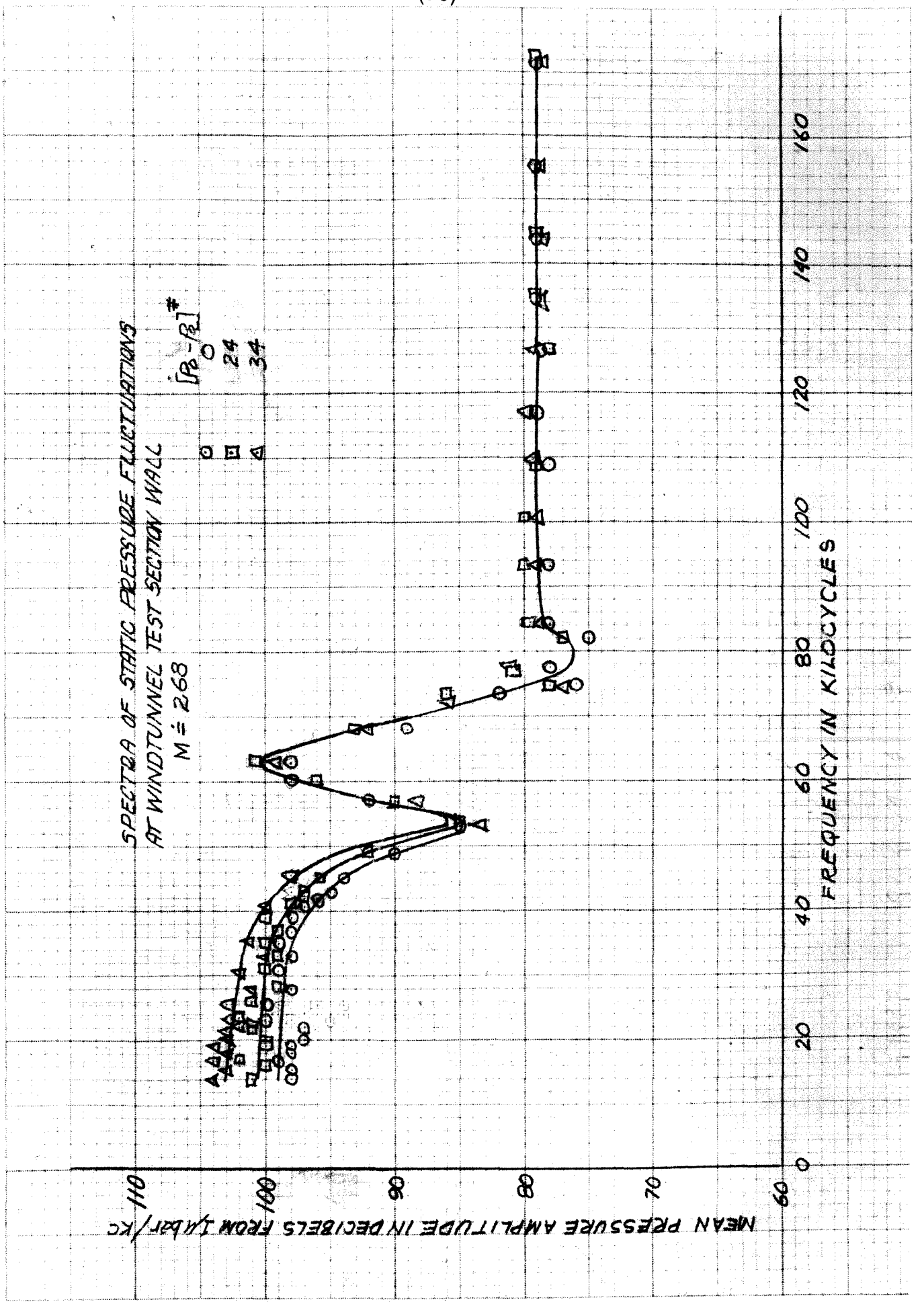
SPECTRA OF STATIC PRESSURE FLUCTUATIONS
AT WINDTUNNEL TEST SECTION WALL
M = 2.68
[PB-P2]* PSF
0
24
34
MEAN PRESSURE AMPLITUDE IN DECIBELS FROM 1 μbar/KC
110
100
90
80
70
60
FREQUENCY IN KILOCYCLES
0
20
40
60
80
100
120
140
160

FIG 12

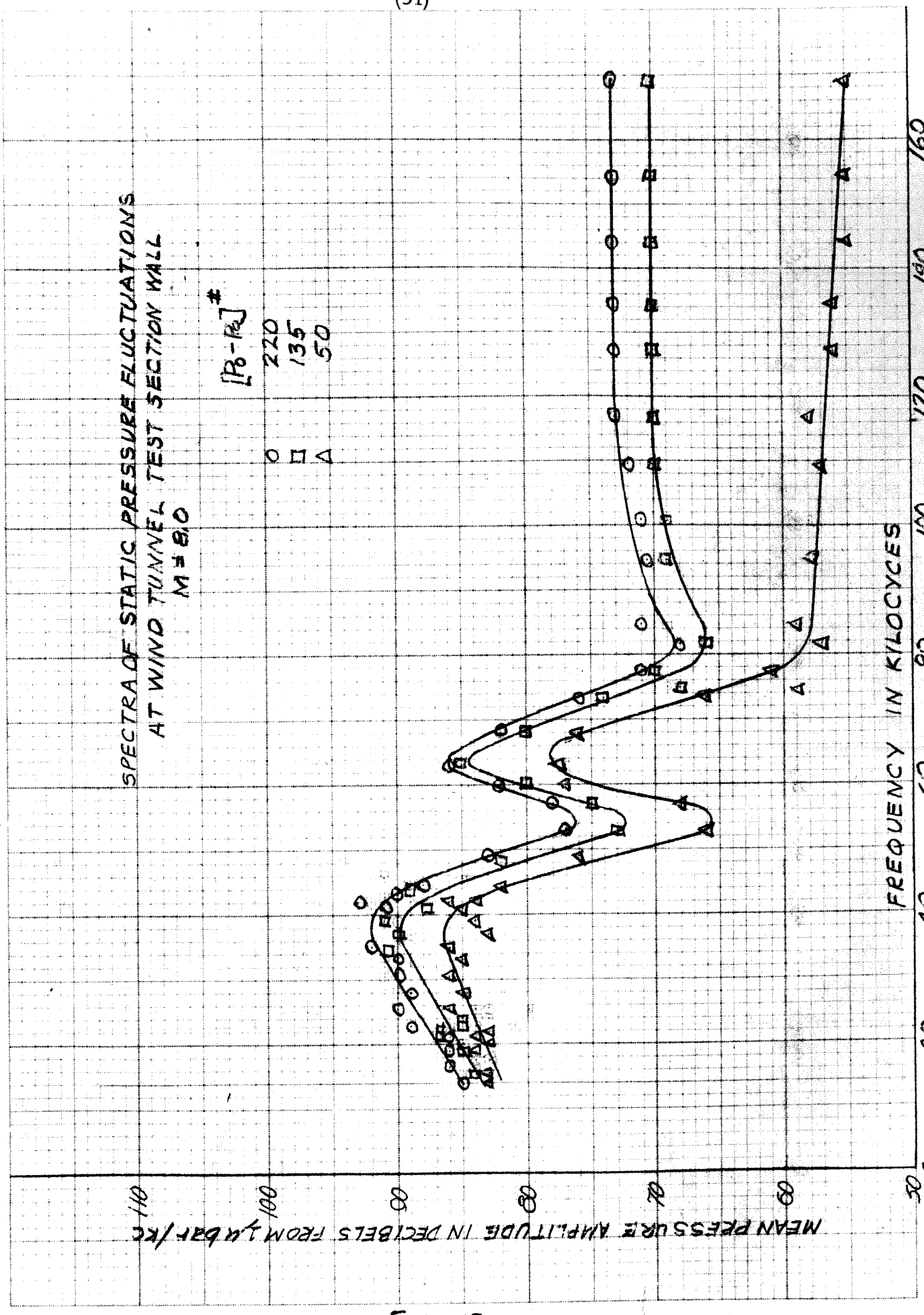
SPECTRA OF STATIC PRESSURE FLUCTUATIONS
AT WIND TUNNEL TEST SECTION WALL
M = 8.0
[Po - Pa]*
220
135
50
MEAN PRESSURE AMPLITUDE IN DECIBELS FROM 1 μbar/RC
FREQUENCY IN KILOCYCES
0
20
40
60
80
100
120
140
160
180
200

FIG 13

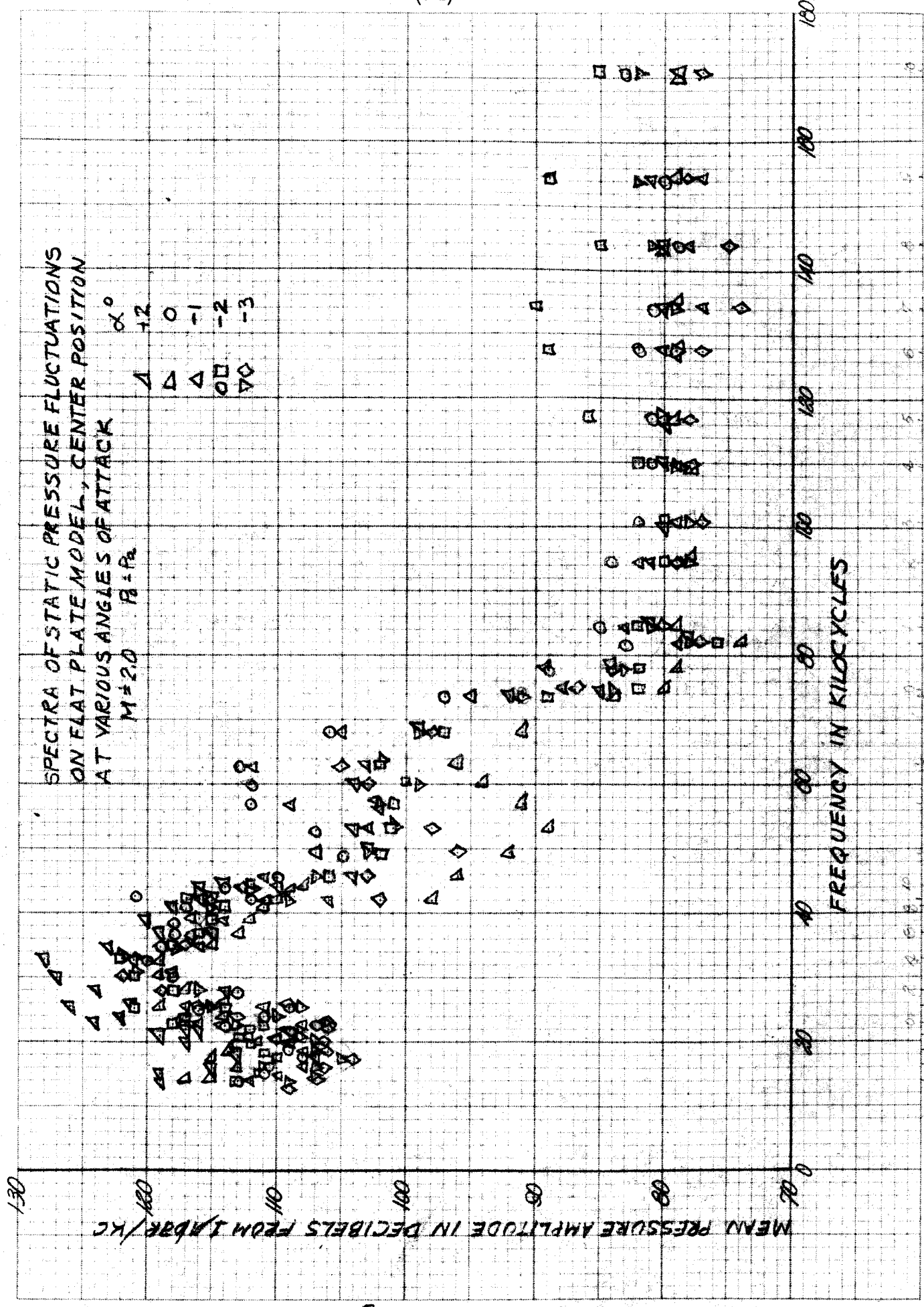
SPECTRA OF STATIC PRESSURE FLUCTUATIONS
ON FLAT PLATE MODEL, CENTER POSITION
AT VARIOUS ANGLES OF ATTACK
M = 2.0 P0 = P2
α°
+2
-1
-2
-3
MEAN PRESSURE AMPLITUDE IN DECIBELS FROM 1 MBAR/KC
FREQUENCY IN KILOCYCLES
130
120
110
100
90
80
70
0
20
40
60
80
100
120
140
160
180

FIG 14

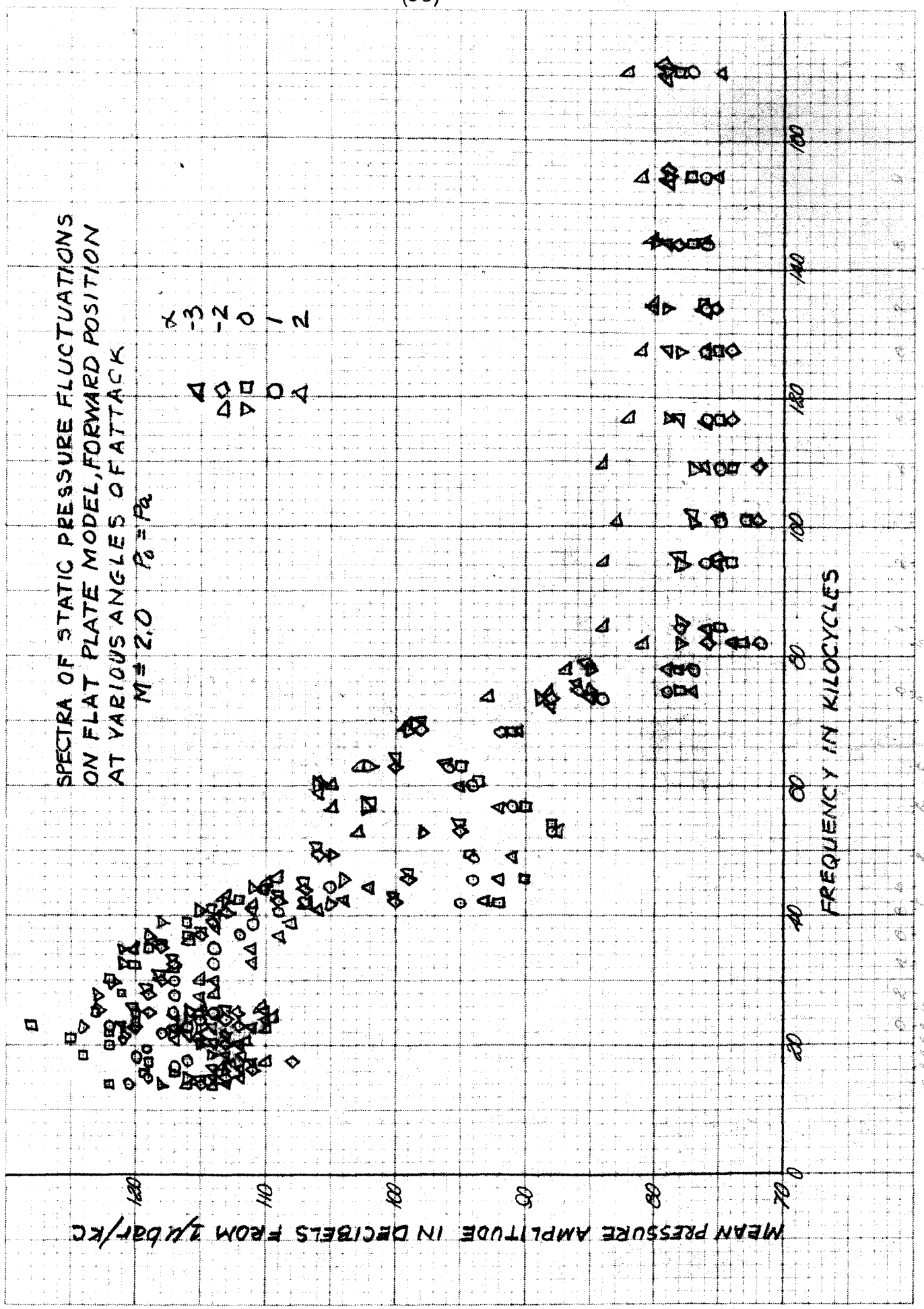
SPECTRA OF STATIC PRESSURE FLUCTUATIONS
ON FLAT PLATE MODEL, FORWARD POSITION
AT VARIOUS ANGLES OF ATTACK
M = 2.0 P₀ = P₀
α
-3
-2
0
1
2
MEAN PRESSURE AMPLITUDE IN DECIBELS FROM 1 μ bar/KC
120
110
100
90
80
70
0
20
40
60
80
100
120
140
160
FREQUENCY IN KILOCYCLES

FIG 15

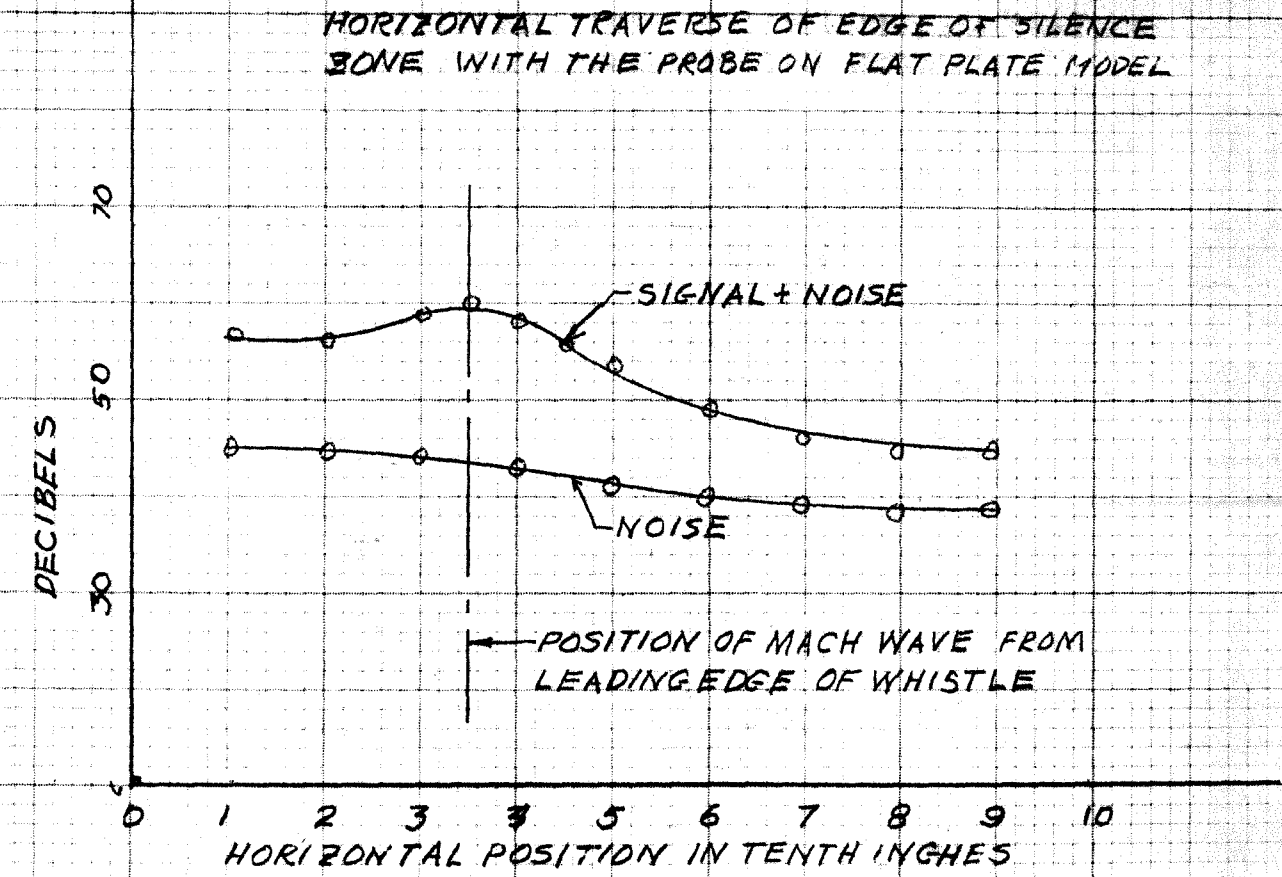
HORIZONTAL TRAVERSE OF EDGE OF SILENCE ZONE WITH THE PROBE ON FLAT PLATE MODEL
SIGNAL + NOISE
NOISE
POSITION OF MACH WAVE FROM LEADING EDGE OF WHISTLE
DECIBELS
70
50
30
0 1 2 3 4 5 6 7 8 9 10
HORIZONTAL POSITION IN TENTH INCHES

FIG. 16

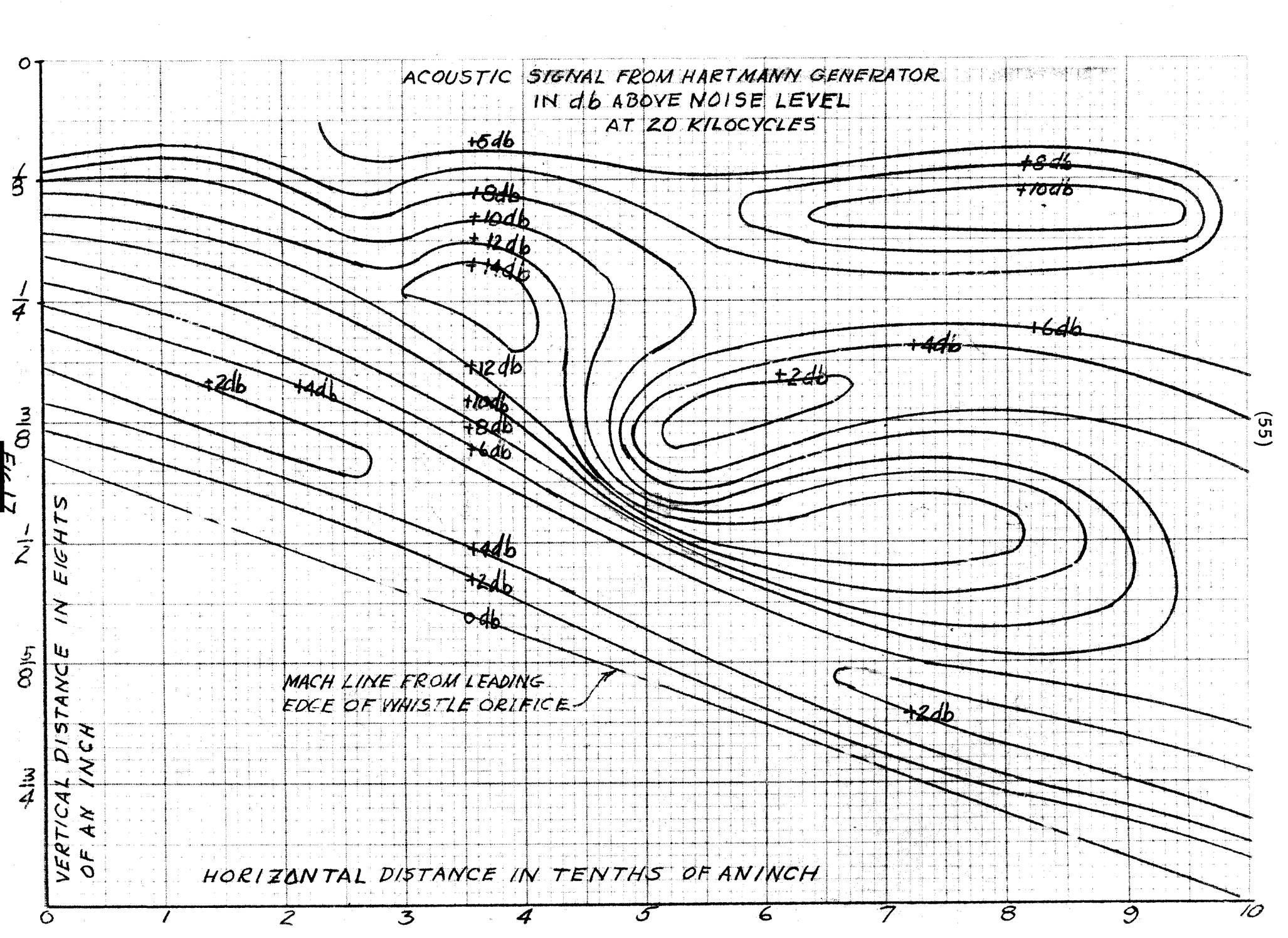
ACOUSTIC SIGNAL FROM HARTMANN GENERATOR
IN db ABOVE NOISE LEVEL
AT 20 KILOCYCLES
+6db
+8db
+10db
+12db
+14db
+8db
+10db
+12db
+10db
+8db
+6db
+4db
+2db
+6db
+4db
+2db
+4db
+2db
0db
+2db
MACH LINE FROM LEADING
EDGE OF WHISTLE ORIFICE
VERTICAL DISTANCE IN EIGHTS
OF AN INCH
HORIZONTAL DISTANCE IN TENTHS OF AN INCH
0
1
2
3
4
5
6
7
8
9
10